AD_____

Award Number:  DAMD17-03-1-0019


TITLE:  Incorporating Model Parameter Uncertainty into Prostate IMRT Treatment Planning


PRINCIPAL INVESTIGATOR:  David Y. Yang, Ph.D.
                         Jun Lian, Ph.D.


CONTRACTING ORGANIZATION:  Stanford University
                           Stanford, California  94305-5401


REPORT DATE:  April 2004


TYPE OF REPORT:  Annual Summary


PREPARED FOR:  U.S. Army Medical Research and Materiel Command
               Fort Detrick, Maryland  21702-5012

20041101 057

**BEST AVAILABLE COPY**

# REPORT DOCUMENTATION PAGE

| 1. AGENCY USE ONLY (Leave blank) | 2. REPORT DATE April 204 | 3. REPORT TYPE AND DATES COVERED Annual Summary (1 Apr 2003 - 31 Mar 2004) |
|---|---|---|

**4. TITLE AND SUBTITLE**
Incorporating Model Parameter Uncertainty into Prostate IMRT Treatment Planning

**5. FUNDING NUMBERS**
DAMD17-03-1-0019

**6. AUTHOR(S)**
David Y. Yang, Ph.D.
Jun Lian, Ph.D.

**7. PERFORMING ORGANIZATION NAME(S) AND ADDRESS(ES)**
Stanford University
Stanford, California 94305-5401

E-Mail: JunLian@med.unc.edu

**8. PERFORMING ORGANIZATION REPORT NUMBER**

**9. SPONSORING / MONITORING AGENCY NAME(S) AND ADDRESS(ES)**

U.S. Army Medical Research and Materiel Command
Fort Detrick, Maryland 21702-5012

**10. SPONSORING / MONITORING AGENCY REPORT NUMBER**

**11. SUPPLEMENTARY NOTES**
Original contains color plates: All DTIC reproduction will be in black and white.

**12a. DISTRIBUTION / AVAILABILITY STATEMENT**
Approved for Public Release; Distribution Unlimited

**12b. DISTRIBUTION CODE**

**13. ABSTRACT (Maximum 200 Words)**

Radiobiological treatment planning depends not only on the accuracy of the models describing the dose-response relation of different tumors and normal tissues but also on the accuracy of tissue specific radiobiological parameters in these models. Whereas the general formalism remains the same, different sets of model parameters lead to different solutions and thus critically determine the final plan. Here we describe an inverse planning formalism with inclusion of model parameter uncertainties. This is made possible by using a statistical analysis-based frameset developed by our group. In this formalism, the uncertainties of model parameters, such as the parameter a that describes tissue-specific effect in EUD model, are expressed by probability density function and are included in the dose optimization process. We found that the final solution strongly depends on distribution functions of the model parameters. Considering that currently available models for computing biological effects of radiation are simplistic, and the clinical data used to derive the models are sparse and of questionable quality, the proposed technique provides us with an effective tool to minimize the effect caused by the uncertainties in a statistical sense. With the incorporation of the uncertainties, the technique has potential for us to maximally utilize the available radiobiology knowledge for better IMRT treatment.

**14. SUBJECT TERMS**
Biological model, radiation therapy, uncertainty

**15. NUMBER OF PAGES**
59

**16. PRICE CODE**

| 17. SECURITY CLASSIFICATION OF REPORT | 18. SECURITY CLASSIFICATION OF THIS PAGE | 19. SECURITY CLASSIFICATION OF ABSTRACT | 20. LIMITATION OF ABSTRACT |
|---|---|---|---|
| Unclassified | Unclassified | Unclassified | Unlimited |

# Table of Contents

# I. INRTODCUCTION

The postdoctoral fellowship grant was awarded to the principal investigator (PI) for the period of April 1, 2003—March 31, 2005. The purpose of this investigation is to introduce a framework for including model parameter uncertainties into prostate Intensity Modulation Radiation Therapy (IMRT) dose optimization so that biological model-based objective function can be used with improved confidence level. The specific aims of the proposal are: (1) to establish a mathematical formalism to incorporate model parameter uncertainty into IMRT optimization; (2) to identify the clinically relevant biological model parameter variance range; and (3) to study the prostate cancer treatment planning including the model uncertainty information. Under the generous support from the U.S. Army Medical Research and Materiel Command (AMRMC), the PI has contributed significantly to the radiation treatment of prostate cancer. Several conference abstracts and refereed papers have been resulted from the support. The project is integrated with ongoing radiation treatment so that the PI has obtained clinical experience while accomplishing the proposed projects. The preliminary data and clinical training obtained under the support of this grant has enabled the PI to start as an assistant professor in the Department of Radiation Oncology at a prestigious university.

# II. RESEARCH AND ACCOMPLISHMENTS

Adenocarcinoma of the prostate has become the most common malignancy in men in the western countries. Options for active management of organ-confined prostate cancer include radical prostatectomy and definitive radiotherapy with either external beams or interstitial brachytherapy. Intensity Modulated Radiation Therapy (IMRT) is quickly replacing conventional techniques for the treatment of prostate cancer. Most IMRT optimization systems at present use dose and/or dose volume-based objective functions [1], which guide the IMRT planning by imposing a penalty according to the difference between the computed and prescribed doses. A well-known drawback of the dose-based inverse planning is that the nonlinear dose response of tumor or normal structures is not fully considered. A number of mathematical models have been developed over the years to better describe the biological effect of radiation and considerable works have also been done to use these biological models to construct more meaningful objective functions for therapeutic dose optimization [2]. Generally speaking, radiobiological formalism involves the use of model parameters that are of considerable uncertainty [3-5]. For instance, the radiosensitivity $\alpha$ of Webb's TCP model varies from 0.157 $Gy^{-1}$ to 0.090 $Gy^{-1}$ when model parameters were fit to 103 patients' data [3]. Biological 'margins' have been used to account for the variability in radiation sensitivity. Similar to the use of a safety margin to account for the potential uncertainties in targeting a tumor, this method assigns more conservative radiosensitivity values to the tumor or sensitive structures to deal with the potential uncertainty of the parameter[6].

The purpose of this project is to develop a framework to include any types of model parameter uncertainties to the dose optimization. In our approach, the uncertainty of a model parameter is quantified by a probability density function and its influence is then incorporated into inverse planning through the use of a statistical inference theorem [7]. Our model is formulated on the equivalent uniform dose (EUD) [8, 9]:

$$EUD = \left( \frac{1}{N} \sum_i D_i^a \right)^{\frac{1}{a}}$$

(1)

for both tumor and normal tissues, where $N$ is the number of voxels in the structure, $D_i$ is the dose delivered to the $i$th voxel, $a$ is the tumor or normal tissue-specific parameter that describes the dose-volume effect. The corresponding objective function to measure the goodness of a dose distribution is given by [9]

$$F = \prod_j f_j$$

(2)

where the component subcore $f_j$ may be either

4

$$f_T = \frac{1}{1 + \left(\dfrac{EUD_0}{EUD}\right)^n}$$

(3)

for tumors, or

$$f_{OAR} = \frac{1}{1 + \left(\dfrac{EUD}{EUD_0}\right)^n}$$

(4)

for normal tissues and organs at risk (OARs). $EUD_0$ is the desired dose parameter for the target volume and the maximum tolerable uniform dose for normal structures. Parameter $n$ is akin to the structure specific importance factor [10] in the conventional inverse planning formalism that parameterizes our tradeoff strategy of different structure.

We assume that $a_k$ in the EUD model varies according to a simple Gaussian distribution

$$P_n(a_k) = P'_{0n} \exp\{-r_n[a_k - a_0]^2\},$$

(5)

where $a_0$ is the mean value, $P'_{0n}$ is a normalization constant and $a_k$ is one of the sampling values of $a$. For a given distribution, the EUD and the corresponding figure of merit of an IMRT plan vary with the sampling of $a$. We thus rewrite Eqs. (3) and (4) as conditional probabilities for a sampled $a_k$:

$$P_T(EUD \mid a_k) = \frac{1}{1 + \left(\dfrac{EUD_0}{EUD}\right)^n},$$

(6)

$$P_{OAR}(EUD \mid a_k) = \frac{1}{1 + \left(\dfrac{EUD}{EUD_0}\right)^n}.$$

(7)

The objective function for a structure $m$ in the presence of uncertainty in $a$ is expressed as the summation of a series of joint probabilities

$$P_m(EUD) = \sum_k P_m(EUD \mid a_k) \cdot P_m(a_k),$$

(8)

and the overall objective function $P$ of the system is a product of $P_m(EUD)$ defined in Eq. (8). That is

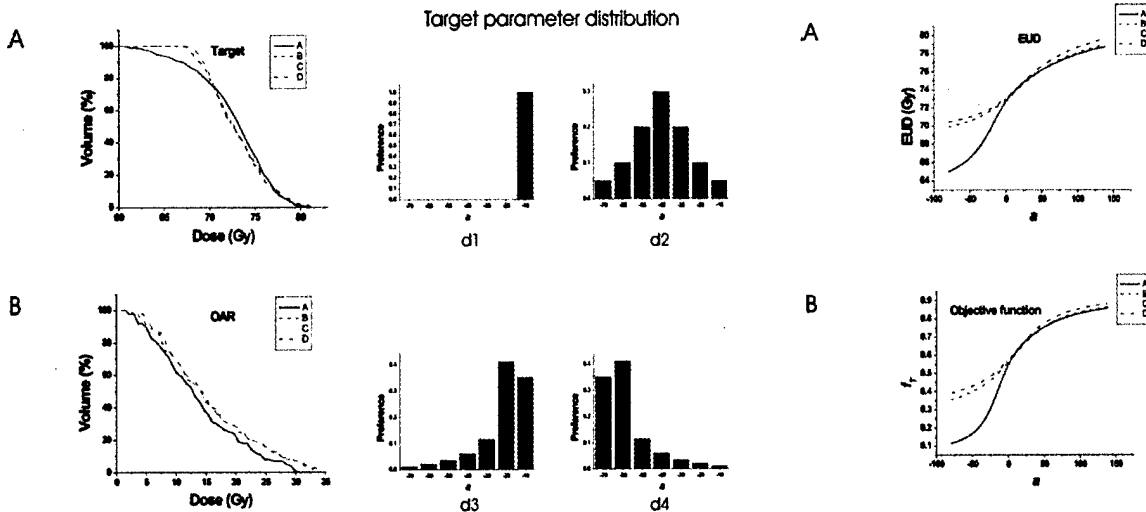$$F = \ln(1/P) = -\ln \prod_m P_m(EUD) = -\sum_m \ln \sum_k P_m(EUD \mid a_k) \cdot P_m(a_k)$$

(9)



Figure 1 (Left) The target and OAR DVHs of four optimal plans when parameter $a$ is a fixed value (bar chart d1) and varies according to three different probabilistic distributions (bar chart d2, d3 and d4).

Figure 2 (Right) The EUD of the target and objective function when parameter $a$ is prescribed according to Fig. 1.

We first investigated the behavior of the system using a C-shaped tumor case when the parameter $a$ of the target EUD takes four different distributions, as depicted in the bar charts shown on the right of Fig. 1, while keeping the parameter $a$ of the OAR at a constant $a_0 = 6.0$. In the case shown in Fig. 1 d1, the parameter $a$ takes only a single value, $a_0 = -10$, which is a simple case studied by Wu et al [9]. The optimal plans for the four distributions of parameter $a$ differ significantly, as indicated by the target and OAR DVHs shown in Fig. 1 A and B. To estimate the degree of sensitivity of the solutions against a variation in $a$, we computed the target EUD and the objective function, $f_T$, as a function of parameter $a$ for the four optimal dose distributions under different types of uncertainty distributions. The results are plotted in Fig. 2. The results suggest that the EUD becomes much less sensitive to the variation in parameter $a$ in the plans obtained with some "built-in" distributions in parameter $a$ (i.e., plans corresponding to Figs. 1 d2 to d4).

Four IMRT plans with different types of pre-assumed uncertainties were generated for a prostate tumor case (Fig. 3A). These include: (i) The $a$-parameters for both prostate target and OARs are restricted to single values as listed in
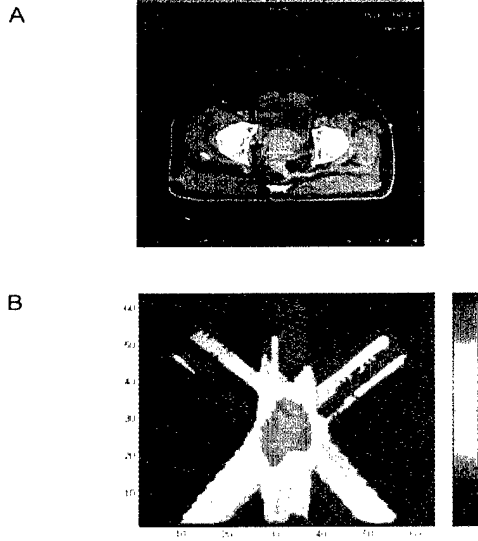
Figure 3. A transverse slice showing the anatomical structures delineated for the prostate tumor (A) and the corresponding optimized dose distribution with the parameters listed in Tab. 1 and the probabilistic distribution shown in Fig. 4B.

Table 1. This plan serves as a reference whose DVHs are shown in Figs. 4A-C as dotted curves; (ii) Only the $a$-parameter of the prostate target takes a range of values, as depicted in the right of Fig. 4A; (iii) Only the $a$-parameter of the rectum takes a range of values, as depicted in the right of Fig. 4B; and (iv) The $a$-parameters of both prostate target and the rectum were allowed to take a range of values, as depicted in the right of Fig. 4C.

DVHs for the plan using parameters defined in Table 1 are plotted with dotted curves and plans with the inclusion of parameter uncertainty are drawn with solid curves (Fig. 4). When the parameter $a$ in target EUD takes a Poisson distribution as shown in the bar chart of Fig. 4A, prostate dose homogeneity is significantly improved. The minimum dose increases from 55 Gy to 67 Gy, and the maxim dose decreases slightly from 82 Gy to 80Gy. However the volumes receiving radiation dose for rectum, bladder and normal tissue all increase significantly though the maximum dose remains similar. The improvement of the target coverage and compromise of OAR sparing is a natural outcome of the competitive requirements for targets and OARs imposed on the system. The corresponding dose distribution with the target
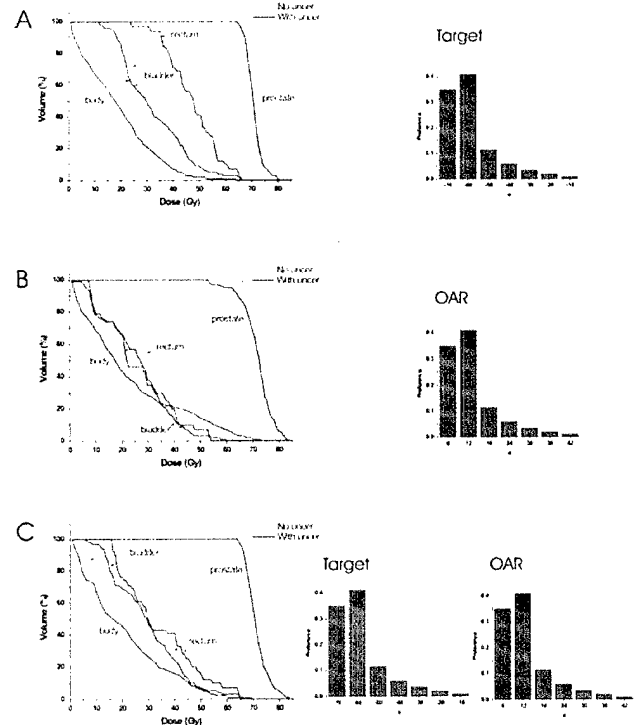
Figure 4. DVHs for a prostate cancer case using the conventional optimization with fixed $a$-value (dotted line) and the newly proposed approach with the inclusion of model parameter uncertainty (solid line). (A) Only the $a$-parameter for the target is assigned with a probabilistic distribution; (B) Only the $a$-parameter for the OAR is assigned with a probabilistic distribution; (C) Uncertainties in the $a$-parameter are introduced for both the target and OAR.

6

corresponding dose distribution with the target parameter defined in the bar chart A is shown in Fig. 3B. Next we considered the inclusion of parameter $a$ uncertainty in EUD calculation in one of the critical structures-rectum (Fig. 4 B). The irradiated rectum volume for a dose below 60 Gy is less than that of a conventional plan with the parameter $a$ fixed at 24. DVHs for the bladder, normal tissue and prostate do not change significantly compared to the plan without inclusion of parameter uncertainty. Lastly, we simultaneously replaced target and rectum parameters with the distributions shown in Fig. 4 C. Similar to that corresponds the prescription of Fig. 4 A, the prostate coverage is improved. However, the rectum DVH in this case is not worsen greatly because parameter $a$ of rectum EUD was allowed to take a spectrum of values. For bladder and normal tissue, although their irradiated volumes in the low dose region are higher than those of the conventional plan, the volumes receiving high doses are reduced.

Table 1. The conventional EUD-based optimization parameter for prostate cancer.

|  | PTV | PTV* | Bladder | Rectum | NT |
| --- | --- | --- | --- | --- | --- |
| a | -10.0 | 10.0 | 6.0 | 24 | 6.0 |
| $EUD_0$(Gy) | 72 | 76 | 35 | 35 | 35 |
| n | 20 | 20 | 6 | 6 | 6 |

* Contains parameters for the target treated as virtual normal tissue to limit dose inhomogeniety.

## III. KEY RESEARCH ACCOMPLISHMENTS

• Developed a series of mathematical formulae to incorporate model parameter uncertainty into IMRT optimization.

• Verified the new method in the prostate cancer case and better dose coverage/sparing can be obtained with appropriate parameters.

## IV. REPORTABLE OUTCOMES

The following is a list of publications resulted from the grant support. Copies of the publication materials are enclosed with this report.

*Refereed publication:*
1. Lian J., Cotrutz C. and Xing L. Therapeutic treatment plan optimization with probability density-based dose prescription. Medical Physics 30: 655-666 (2003).
2. Lian J. and Xing L. Incorporating Model Parameter Uncertainty into Inverse Treatment Planning, Medical Physics, (tentatively accepted), 2004.

*Published Abstracts:*
1. Lian J., Spielman D., Cotrutz C., Hunjan S., Adalsteinsson E., King C., Luxton G., Kim D., Daniel B. and Xing L. Including metabolic uncertainty into proton MR spectroscopic imaging (MRSI)-guided inverse treatment planning. In: the 45th American Association of Physicists in Medicine (AAPM) Meeting, San Diego, 2003
2. Lian J. and Xing L. Biological Model Based IMRT Optimization with Inclusion of Parameter Uncertainty. In: the 14th International Conference on the Use of Computers in Radiation Therapy (ICCR), Seoul, Korea, 2004

*New Employment:*
With the help of this grant and associated publications, PI has obtained an assistant professor position in the Department of Radiation Oncology at the University of North Carolina at Chapel Hill.

# V. CONCLUSIONS

A technique for incorporating biological model parameter uncertainties into inverse treatment planning has been developed. The formalism is quite general and does not prerequisite the specific form of uncertainty distributions of the involved model parameters. By including model parameter uncertainties, the final solution becomes more robust and the treatment outcome will be less likely influenced by inter-patient variation of biological characteristics. With the increasing interest in radiation therapy community to use biologically based models for treatment planning, this work provides an effective way to better account for the known uncertainties in the model parameters and allows us to maximally utilize the available radiobiology knowledge to facilitate patient care.

## References

1    Q. Wu and R. Mohan, Algorithms and functionality of an intensity modulated radiotherapy optimization system. Med Phys. **27**, 701-11 (2000).

2    A. Brahme, J. Nilsson, and D. Belkic, Biologically optimized radiation therapy. Acta Oncol. **40**, 725-34 (2001).

3    S. Levegrun, A. Jackson, M.J. Zelefsky, M.W. Skwarchuk, E.S. Venkatraman, W. Schlegel, Z. Fuks, S.A. Leibel, and C.C. Ling, Fitting tumor control probability models to biopsy outcome after three-dimensional conformal radiation therapy of prostate cancer: pitfalls in deducing radiobiologic parameters for tumors from clinical data. Int J Radiat Oncol Biol Phys. **51**, 1064-80 (2001).

4    J.D. Fenwick, Predicting the radiation control probability of heterogeneous tumour ensembles: data analysis and parameter estimation using a closed-form expression. Phys Med Biol. **43**, 2159-78 (1998).

5    J.O. Deasy, K.S. Chao, and J. Markman, Uncertainties in model-based outcome predictions for treatment planning. Int J Radiat Oncol Biol Phys. **51**, 1389-99 (2001).

6    A. Brahme, Optimized radiation therapy based on radiobiological objectives. Semin Radiat Oncol. **9**, 35-47 (1999).

7    L. Xing, J.G. Li, A. Pugachev, Q.T. Le, and A.L. Boyer, Estimation theory and model parameter selection for therapeutic treatment plan optimization. Med Phys. **26**, 2348-58 (1999).

8    A. Niemierko, Reporting and analyzing dose distributions: a concept of equivalent uniform dose. Med Phys. **24**, 103-10 (1997).

9    Q. Wu, R. Mohan, A. Niemierko, and R. Schmidt-Ullrich, Optimization of intensity-modulated radiotherapy plans based on the equivalent uniform dose. Int J Radiat Oncol Biol Phys. **52**, 224-35 (2002).

10   L. Xing, J.G. Li, S. Donaldson, Q.T. Le, and A.L. Boyer, Optimization of importance factors in inverse planning. Phys Med Biol. **44**, 2525-36 (1999).

## Appendix. Copies of manuscripts and Abstracts (see attachment)

# Therapeutic treatment plan optimization with probability density-based dose prescription

Jun Lian, Cristian Cotrutz, and Lei Xing[a]
*Department of Radiation Oncology, Stanford University School of Medicine, 300 Pasteur Drive, Stanford, California 94305-5304*

The dose optimization in inverse planning is realized under the guidance of an objective function. The prescription doses in a conventional approach are usually rigid values, defining in most instances an ill-conditioned optimization problem. In this work, we propose a more general dose optimization scheme based on a statistical formalism [Xing *et al.*, Med. Phys. **21**, 2348–2358 (1999)]. Instead of a rigid dose, the prescription to a structure is specified by a preference function, which describes the user's preference over other doses in case the most desired dose is not attainable. The variation range of the prescription dose and the shape of the preference function are predesigned by the user based on prior clinical experience. Consequently, during the iterative optimization process, the prescription dose is allowed to deviate, with a certain preference level, from the most desired dose. By not restricting the prescription dose to a fixed value, the optimization problem becomes less ill-defined. The conventional inverse planning algorithm represents a special case of the new formalism. An iterative dose optimization algorithm is used to optimize the system. The performance of the proposed technique is systematically studied using a hypothetical C-shaped tumor with an abutting circular critical structure and a prostate case. It is shown that the final dose distribution can be manipulated flexibly by tuning the shape of the preference function and that using a preference function can lead to optimized dose distributions in accordance with the planner's specification. The proposed framework offers an effective mechanism to formalize the planner's priorities over different possible clinical scenarios and incorporate them into dose optimization. The enhanced control over the final plan may greatly facilitate the IMRT treatment planning process. © *2003 American Association of Physicists in Medicine.*
[DOI: 10.1118/1.1561622]

Key words: IMRT, dose optimization, inverse planning, statistical analysis

## I. INTRODUCTION

Inverse planning is used in intensity modulated radiation therapy (IMRT) for deriving the optimal beam intensity profiles that produce the best possible dose distribution for a given patient.[1–16] The dose optimization process is usually performed under the guidance of an objective function, which measures the "distance" between the physical and the prescribed dose distributions.[8,17–20] One of the common objective functions for inverse planning is the quadratic objective function,[3,21,22] with importance factors assigned to the involved structures to prioritize their relative importance during the optimization process.[23–25] The objective function is defined as a global quantity based on general physical considerations. When the desired dose distribution is not attainable during optimization, a compromise solution is found using the algorithm's ranking. The compromise dose distribution, however, is often not what the planner wants and multiple trial and errors are needed to obtain a clinically acceptable IMRT plan.

A main problem of the existing IMRT planning algorithms is the lack of an effective mechanism for incorporating prior knowledge into inverse planning.[31] In the past, there have been many attempts to introduce soft/hard constraints to steer the dose optimization process toward the clinically desired solutions.[26–30,36] However, the constraints are introduced in an *ad hoc* fashion and do not fully utilize the partial information available from years of clinical investigations because of their phenomenological nature. On a more fundamental level, the constraints are imposed *a posteriori* and controls the optimization passively. Our purpose in this paper is to develop a statistical analysis-based inverse planning formalism to more effectively utilize the prior knowledge. Instead of specifying a rigid prescription dose, the formalism allows us to use a dose distribution as the input prescription to the system, providing a natural way for us to take advantage of the existing information of the system variables and promising to make the optimization outcome more predictable and controllable.

In the next section we present the details of the new dose optimization algorithm after a brief introduction of the concept of preference function. The formalism is then applied to a synthetic phantom case with C-shaped tumor target and a prostate case. Our results indicate that the statistical analysis-based formalism provides a general framework for inverse planning and is capable of producing conformal IMRT dose distribution. Coupled with the capability of the preference function in customizing/formalizing our prior clinical knowledge, it is expected that the proposed technique will have a

broad implication and potential to greatly facilitate an IMRT planning process.

## II. MATERIAL AND METHODS

### A. Theoretical background

In a vectorial form, the dose to the points in the treatment region depend upon the beamlet weights **w** as

$$\mathbf{D}_c = \mathbf{d} \cdot \mathbf{w}, \tag{1}$$

where **d** represents the dose deposition matrix, expressing the dose deposited to any point in the patient when irradiated with a unit weight beamlet vector. The inverse problem as posed for IMRT is to find a set of beamlet weights that produce the optimal dose distribution by minimizing a therapeutic objective function. The most used objective function has a quadratic form and reads[32] as

$$F = \frac{1}{N} \sum_{n=1}^{N} r_\sigma [D_c(n) - D_p(n)]^2, \tag{2}$$

where $N$ is the total number of voxels, $r_\sigma$ is the importance factor that controls the relative importance of a structure $\sigma$, and $D_p$ and $D_c$ are prescribed and calculated doses, respectively.

In inverse planning algorithm based on the quadratic objective function [Eq. (2)], the dose prescription to the target or sensitive structure takes a rigid value. The minimization of the objective function is realized by various algorithms like simulated annealing, gradient methods, etc.[17,26,32,33] Independent of the used dose optimization algorithms, we will call these methods throughout the text conventional IMRT optimization procedures. The problem is usually ill-posed and may lead to negative fluence unless hard constraints are introduced.[3] Practically, it is not uncommon that the plans computed by what are called optimization systems are not consistent with the expectation of the planner and that several trial-and-error adjustments of the system parameters might be required to achieve a clinically acceptable plan. Given a patient, the obtained plan can vary widely from one planer to the next, even within a department. In the following we describe a more adaptable and "intelligent" statistical inverse planning formalism based on the concept of a preference function to better deal with the dilemma.

### B. Preference function

In a recent paper, Xing et al.[31] introduced the concept of preference function to weaken the rigid dose prescription commonly seen in the existing inverse planning algorithms. Its role is to allow a dose distribution to be considered instead of just a single value, and to quantify the degree of our willingness to accept a prescription dose $D_p$ in that range. The preference function can be constructed heuristically from clinical considerations.[31] The defined preference function states that the most favorable prescription dose for a voxel $n$ is $D_p(n)$ and that a different prescription dose is also acceptable, but with a smaller preference level. For illustration, in Fig. 1 we show a sketch of the preference functions
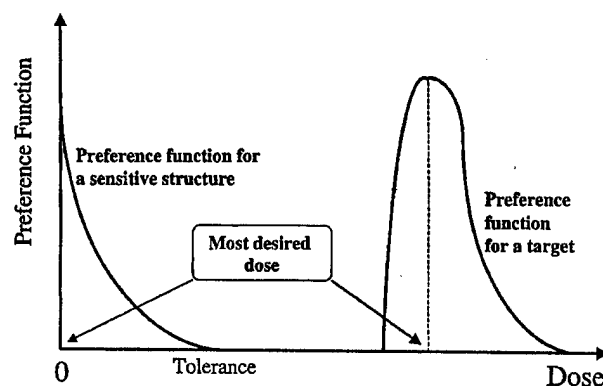


FIG. 1. A sketch of preference functions for a target and a sensitive structure.

for a target and sensitive structure. The most desirable dose for a sensitive structure should generally be set to zero. The conventional prescription scheme represents a special case of the general approach proposed here with the step function form of the preference function. That is,

$$P_n(D_p) = \begin{cases} 1, & \text{if } D_p = D_p^0, \\ 0, & \text{if } D_p \neq D_p^0. \end{cases} \tag{3}$$

To give another example, we write down the Gaussian preference function for a voxel $n$

$$P_n(D_p) = P_{0n} \exp\{- \gamma_n [D_p(n) - D_p^0(n)]^2\}, \tag{4}$$

where $P_{0n}$ is a normalization constant and $\gamma_n$ represents the Gaussian parameter. For a system comprising $N$ voxels, the total preference is given by a product of the preference functions of all voxels:

$$P = \prod_n P_n(D_p)$$

$$= \prod_n P_{0n} \exp\{- \gamma_n [D_p(n) - D_p^0(n)]^2\}. \tag{5}$$

When a maximum likelihood estimator is used, it has been demonstrated that the maximization of the logarithmic function of $P$ or minimization of $\ln(1/P)$, is equivalent to the minimization of the conventional quadratic objective function.[31,34] In this case, the Gaussian parameter $\gamma_n$ in Eq. (5), which commands the "spread" of the Gaussian around $D_p^0$, is equivalent to the importance factor that controls the relative importance of the structure and parametrizes the clinical trade-off strategy.

### C. Probability density-based dose prescription and inverse planning

The objective function defined in Eq. (2) uses a rigid dose, $D_p$. Since in most instances an ideal dose prescription is not physically attainable, we resort to an expansion of the prescription dose, over a certain interval. That is, we allow the prescription dose to take a "probabilistic" distribution around the most desired dose as specified by the preference function. For computational purpose, we divide the permis-

sible prescription dose into a number of discretized values, $\{D_p^i\}$, where $i$ is the index of a possible prescription dose and $i=0$ represents the most desirable dose. The preference distribution prescription is usually normalized to unity.

In order to utilize the probability information characterized by the preference function, we formulate the conventional dose optimization into a statistical analysis problem. To proceed, let us take the quadratic objective function as an example. We rewrite the traditional quadratic objective function (2) into

$$f(D_c) = f_0 \prod_n \exp\{-r_\sigma[D_c(n)-D_p(n)]^2\}. \tag{6}$$

where $f_0$ is a normalization constant. For a given prescribed dose distribution, Eq. (6) measures the goodness of a calculated dose distribution using an exponential scale, as compared with Eq. (2). Equation (6) can be interpreted as a conditional probability and formally rewritten as

$$f(D_c|D_p) = f_0 \prod_n \exp\{-r_\sigma[D_c(n)-D_p(n)]^2\}. \tag{7}$$

When the prescription dose is no longer a rigid dose, it is conceivable that there are a number of optimum solutions, each corresponding to a sample of prescription doses. Mathematically, we now have two "probability" distribution functions. One is the preference function that characterizes our *a priori* preference over different prescription doses $P(D_p)$, and the other is Eq. (6) that ranks a calculated dose for a given prescribed dose, $D_p$. Our task is to find the solution that is statistically optimal with consideration of the variable prescription. For this purpose, we introduce the "joint probability" of the two "probability" distributions defined by Eqs. (5) and (7). The function at a voxel $n$ can be written as

$$P_n(D_c) = \sum_i f_n(D_c|D_p^i)P_n(D_p^i). \tag{8}$$

The total preference function of the system is given by

$$P = \prod_n P_n(D_c). \tag{9}$$

## D. Optimization strategy

Having the rigid prescription $D_p$ in (2) replaced by a range of prescribed doses, $\{D_p^i\}$, the total preference function is now given by Eqs. (8) and (9). For convenience, we define objective function $F=\ln(1/P)$ and derive the optimal solution by minimizing the $F$, which is equivalent to maximize the preference function (9). The objective function now reads as

$$F = \ln(1/P)$$

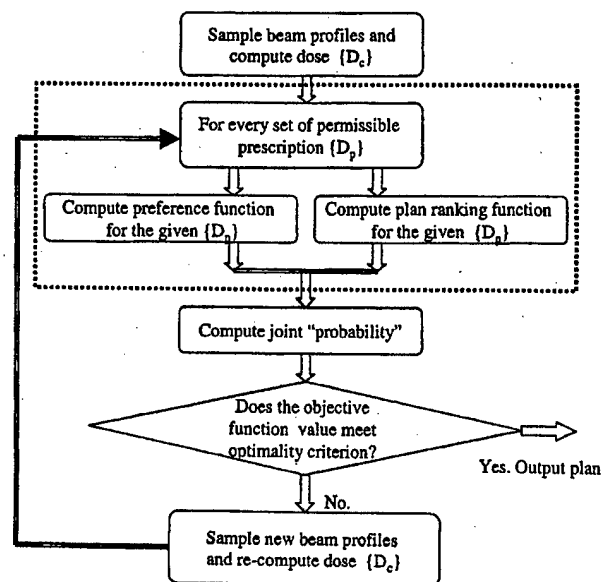$$= -\ln\prod_n P_n = -\sum_n \ln\sum_i f_n(D_c|D_p^i)\cdot P_n(D_p^i). \tag{10}$$

FIG. 2. A flow chart of the optimization process with the inclusion of predesigned preference function information.

Note that the conventional quadratic objective function is a special case of the above general objective function when the prescription takes a rigid value for each structure, as described by Eq. (3).

The optimization process is schematically shown in a flow chart (Fig. 2). The beam profile is determined by minimizing the above objective function using a conjugate gradient optimization algorithm. The details of the algorithm have been discussed in a previous paper.[33] Briefly, the calculation consists of three major steps: (i) assume an initial intensity profile for each incident beam; (ii) compute the "joint probability" given by Eqs. (8) and (9). For this purpose, we need to sample all combinations of the prescription doses of different structures and compute the function given in Eqs. (5) and (7) for each of these combinations; and (iii) optimization of the multidimensional "joint probability" function. The second step is fairly computationally intensive because we must compute the two functions for every sampling of the prescription doses. In our calculation, we typically assign four to seven discrete possible prescription doses for each structure. A finer discretization of the prescription dose did not seem lead to further improvement but would greatly increase the computation time. All calculations presented here are performed on a Personal Computer (PC) with an Intel Pentium® III 1 GHz CPU (Intel Corporation, Sunnyvale, CA). The computation time needed to obtain an optimal solution for a given set of system parameters (including beam configuration, preference function, importance factors) is typically less than ten minutes.

## III. RESULTS AND DISCUSSION

### A. A synthetic phantom case with a C-shaped tumor

To systematically study the performance of the statistical analysis-based inverse planning algorithm, we applied the
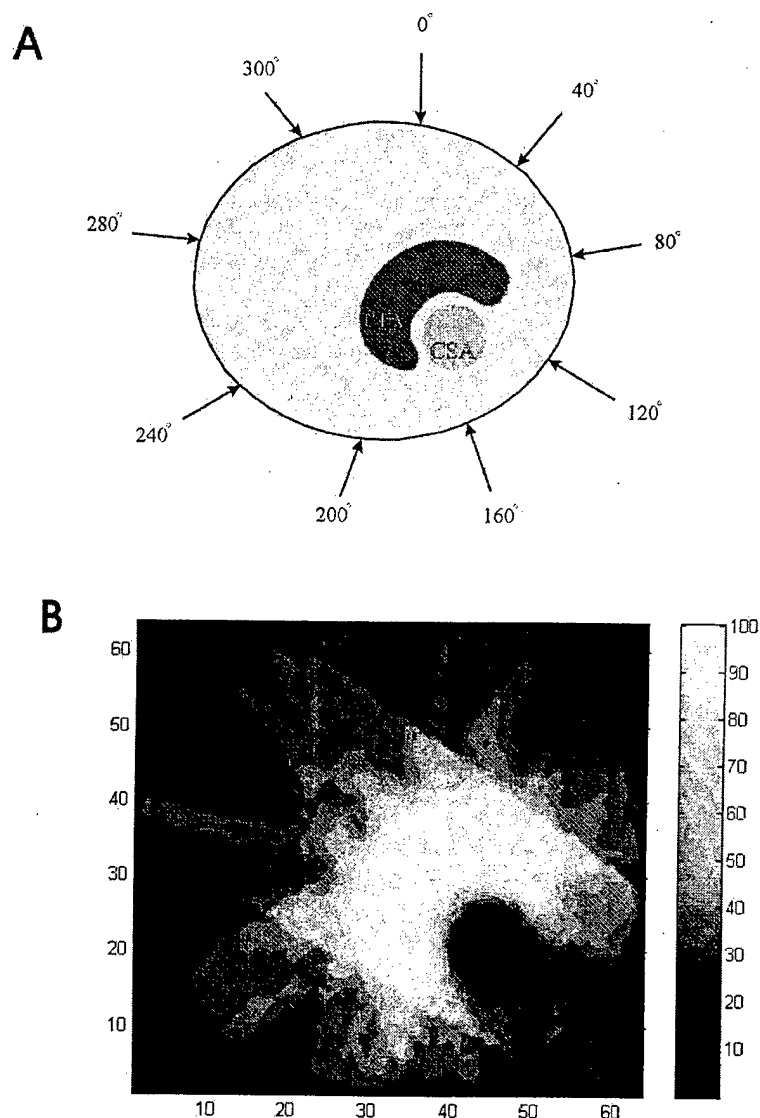
**A**



**B**



FIG. 3. (a) A sketch of a phantom case with a C-shaped tumor. The dose prescription is set 100 (arbitrary units) to the PTV and 0 to the circular OAR and normal tissue. (b) Dose distribution obtained using the "probabilistic" prescription shown in Fig. 4(a).

technique to a C-shaped tumor case [Fig. 3(a)] with a variety of preference functions and compared the results with that obtained using the conventional approach with a fixed dose prescription. Nine equally spaced 6 MV beams beginning at 0° (IEC) were used in this study. The prescription doses to the PTV and OAR in the conventional IMRT plans were 100 and 0 (the dose is in an arbitrary unit), respectively.

We first assigned three sets of symmetrical Gaussian distributions to the target while keeping the prescription to the sensitive structure at zero (Fig. 4). The Gaussian preference functions were represented by three sets of preference levels at seven discrete values (80, 87, 94, 100, 106, 113, and 120). The center of the Gaussian functions was set at 100. The preference levels for the seven doses are shown in Fig. 4 for each of the three situations studied here. The transverse dose distribution obtained using the statistical inverse planning formalism for the case shown in Fig. 4(a) is plotted in Fig. 3(b). As expected, target inhomogeneity increases as we

loosen the constraint of the rigid dose prescription. This can be better demonstrated by using the differential DVH for each situation. As seen from the differential DVH plots (the right column of Fig. 4), the width of the differential function gradually increases, from 26.72, 28.59–30.39, as we gradually increase the acceptance levels for the doses different from the most desirable dose (100). This series of calculations provides us with preliminary evidence that the final dose distribution can be steered by varying the preference function.

Next, we constructed six sets of asymmetric preference functions for the target (Fig. 5 and Fig. 6). When higher preference levels were assigned to the doses higher than 100, we found that the target DVH is shifted to the high dose region. Interestingly, even when an extremely low preference (for instance, 1%) was assigned to the doses less than 100 [Fig. 5(b)], a noticeable underdosing relative to the conventional result was resulted. A similar phenomenon can also be
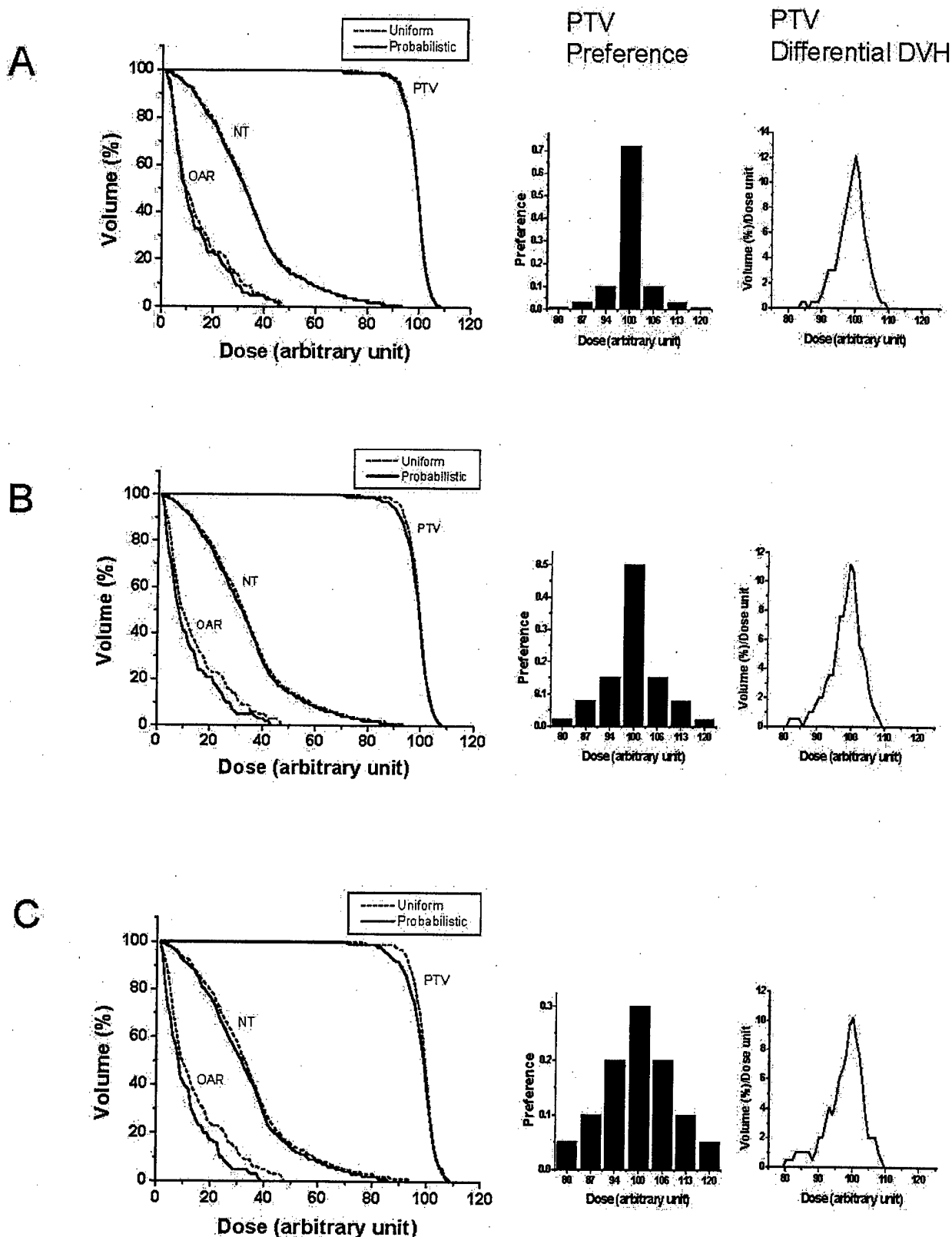
FIG. 4. DVHs of the PTV, OAR, and normal tissue (NT) obtained using the conventional rigid dose prescription (dotted line) and the "probabilistic" prescription (solid line). The Gaussian preference functions with different variances are shown in the middle panel. The right panel shows the differential DVHs for the target.
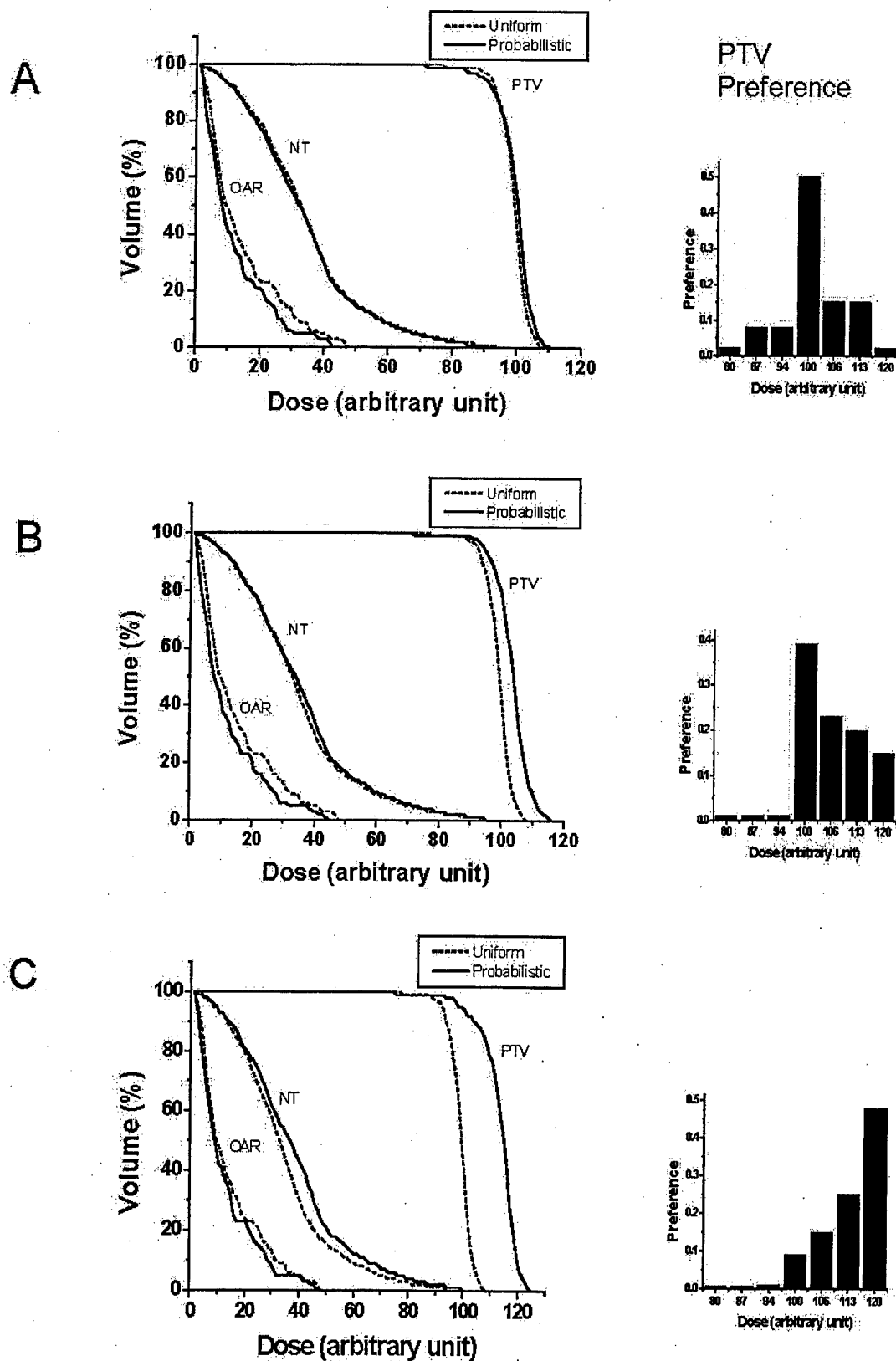
FIG. 5. DVHs of the PTV, OAR, and normal tissue (NT) obtained with the conventional rigid dose prescription (dotted line) and with the "probabilistic" prescription (solid line). The bar charts on right show the asymmetrical preference functions.
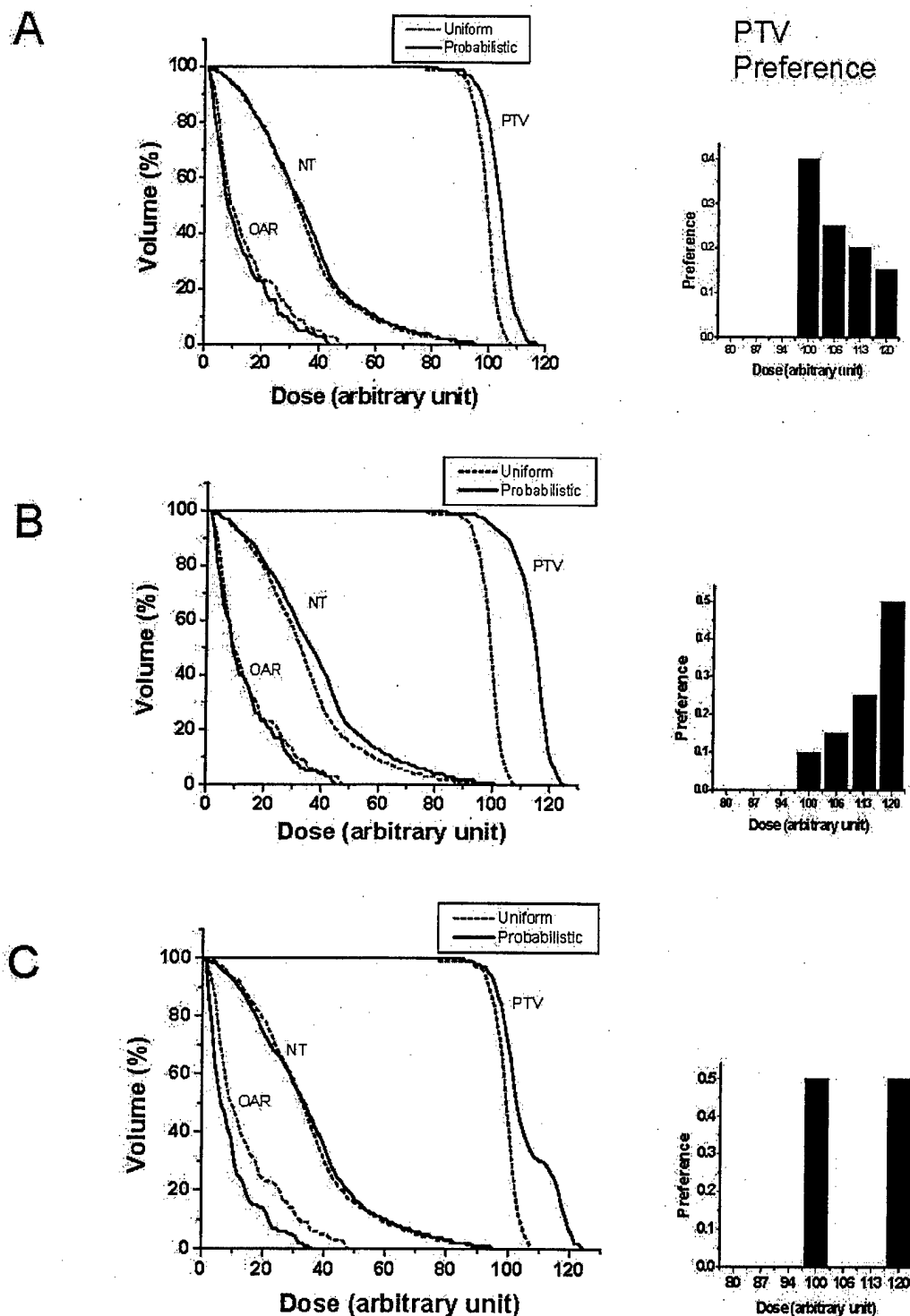
FIG. 6. DVHs of the PTV, OAR, and normal tissue (NT) obtained using the conventional rigid dose prescription (dotted line) and the new statistical inverse planning method for a variety of preference functions shown on the right panel (solid line).

seen from the result shown in Fig. 5(c), where only 0.5%, 0.7%, and 1% of preference levels were assigned to the dose values of 80, 87, and 94. This observation seems to indicate that the influence of the assigned preference level at a low

dose plays an important role. In Fig. 6, we set the preference levels for the doses less than 100 to be 0 and only assign nonzero preference levels for the doses higher than 100. It is seen that in all these situations the minimum target dose is
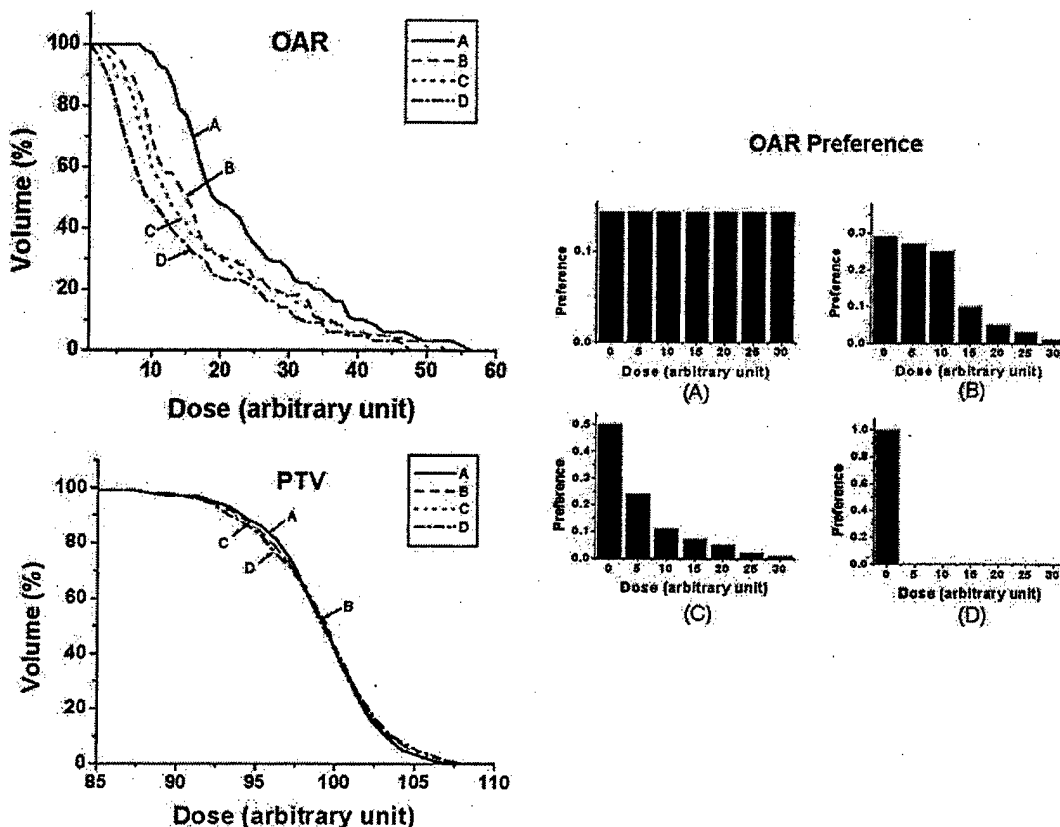
FIG. 7. DVHs of the OAR and PTV when the prescription dose to the OAR is modeled by (a) a uniform distribution, (b) a bell-shaped function, (c) an exponential decay function, and (d) a rigid value.

higher than that of the conventional plan. As a result of our preference over higher doses, the fractional volume at any dose less than 100 is improved in comparison to that of the conventional IMRT plan. In Fig. 6(c), we further exemplify the statistical analysis based inverse planning method by simplifying our preference to two doses (100 and 120), each with 50% preference levels. In this situation, in addition to that the doses in the target are shifted toward higher values, the target DVH exhibits a stepwise behavior: a plateau appears at around 110, which is in the middle of the two prescribed doses.

It is interesting to point out that the OAR sparing is improved as compared with the conventional IMRT plan in most cases studied in Figs. 5 and 6, even when the target dose is escalated. That is, the DVH of the OAR is not always shifted toward higher doses, as would occur if a higher dose is prescribed in a conventional inverse planning system. Instead, the dose to the OAR remained unchanged or even lowered in some cases. A reasonable explanation for the observed phenomenon is that, when a rigid dose prescription is replaced by a range of doses, the system is given more freedom for self-adjustment. As a benefit, a solution with a higher integral target dose and reduced OAR dose can be obtained from the expanded solution space.

We have also studied the behavior of the system when a range of doses is prescribed to the OAR. In this investigation, we kept the target prescription to 100 and allowed the

OAR dose to take seven values: 0, 5, 10, 15, 20, 25, and 30 with the acceptance levels sampled from three different types of prescription distribution: uniform [Fig. 7(a)], bell-shaped [Fig. 7(b)], and exponential [Fig. 7(c)] functions. Figure 7(d) represents the conventional case with zero prescription to the OAR. The corresponding OAR and PTV DVHs are plotted in the left panel of Fig. 7. When the preference was uniformly sampled in the dose interval from 0 to 30, the resultant dose to the OAR was found to be the highest, as indicated by curve A in Fig. 7. The best target dose coverage was achieved in this situation. If the preference to a high dose was reduced, the DVH was gradually shifted to the low dose direction (curves B and C). It is not surprising that the best OAR sparing was achieved in the conventional case where a zero dose was prescribed to the OAR. The target dose homogeneity was slightly improved in all cases when a probabilistic prescription was given to the OAR. Similar to that described in the last paragraph, the results clearly demonstrate that the "probabilistic" prescription allows us to control the OAR dose distribution and indicate the usefulness of the statistic analysis approach.

## B. The prostate case

The new inverse planning algorithm was also applied to study a six filed IMRT prostate treatment [Fig. 8(a)]. Four plans with different types of preference functions were gen-
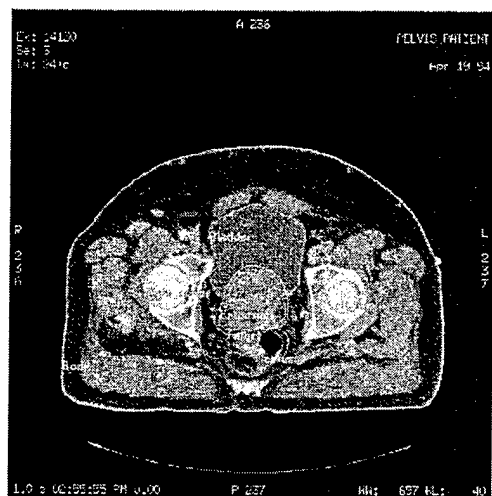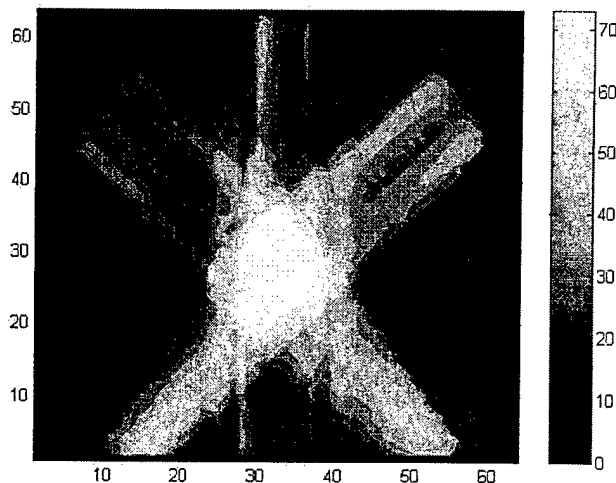
A

B

FIG. 8. A transverse slice showing the anatomical structures delineated for the prostate tumor (a) and (b) the dose distribution obtained using the "probabilistic" prescription shown in Fig. 9(a).

erated. In addition, a plan with rigid prescription (74 Gy on the target, 60 Gy on the bladder, and 40 Gy on the rectum) is also generated. The DVHs for this plan is plotted as dotted lines in Fig. 9 and is used as a reference for comparison. In all treatment plans, six beams were placed at the following angular positions: 0°, 55°, 135°, 180°, 225°, and 305°. The size of the pencil beam defined at the isocenter was 0.5 cm.

The DVH and preference functions for four different plans are schematically shown in Fig. 9. In the study shown in Figs. 9(a)–9(b), we kept the preference function of the sensitive structures unchanged and only varied the form of the preference function of the target. In Fig. 9(a), we assumed that target could take seven discrete values (74, 76, 78, 80, 82, 84, and 86 Gy) sampled from an exponential distribution. Compared with the dotted lines, the target DVH was shifted toward the high dose direction. The dose distribution corresponding to the preference function is shown in Fig. 8(b). The target DVH was shifted even further toward

the high dose region [Fig. 9(b)] when a bell-shaped preference function was used with more emphasis on the target receiving doses at 74, 76, and 78 Gy. In both cases, doses to the rectum and bladder did not change significantly.

In Fig. 9(c) we show the DVHs when the preference function to the rectum deviates from the uniform distribution. As a result, the rectum dose was significantly lowered in all dose levels and the maximum dose was reduced from 66 to 57 Gy. Because of the proximity of the rectum to the prostate target, the maximum rectum dose was not restricted to 30 Gy, as specified in the preference function. We emphasize that the improvement in rectum and bladder sparing was achieved at cost of higher dose inhomogeneity in the prostate target. This reminds us that, in dose optimization, there is a dosimetric compromise. That is, the improvement in the dose to a structure is often accompanied by dosimetrically adverse effect(s) at other points in the same or different structures. The important point that one should note is that from the clinical point
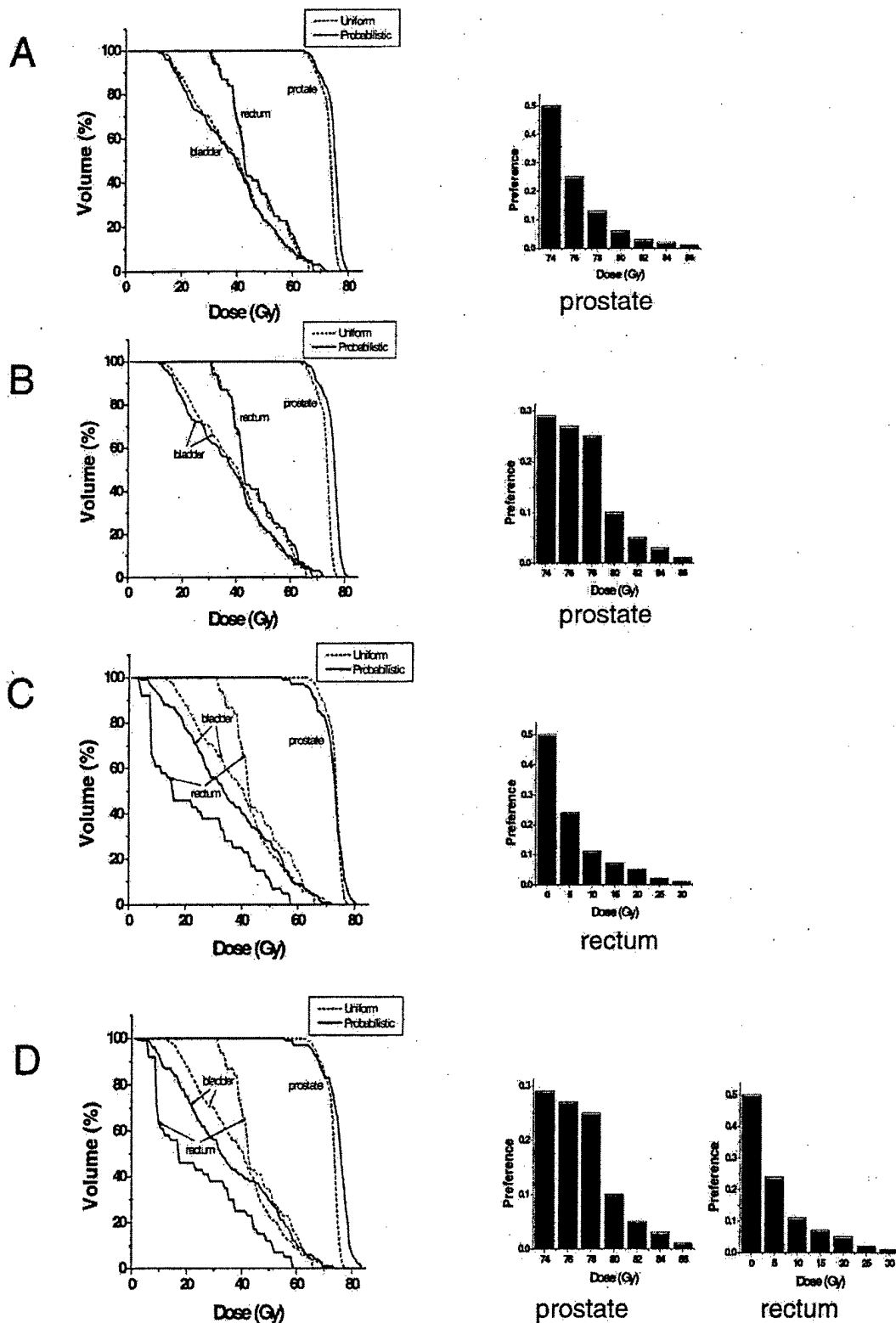
FIG. 9. A comparison of the DVHs obtained using the "probabilistic" prescription (solid line) and conventional rigid dose prescription (dotted line). The prostate and rectum prescriptions are represented on the right bar charts.

of view, some dose distributions are more acceptable than others and our goal is to find the solution that improves the plan to the largest possible extent, but with a clinically insignificant or acceptable sacrifice in OAR sparing. In order to achieve this, it is necessary to have a reasonable amount of controllability over the final dose distribution. In this sense we believe that the proposed formalism is valuable.

In addition, we varied the preference functions for both target and rectum [Fig. 9(d)]. The preference function for the rectum was the same as that in Fig. 9(c). Compared to the results shown in Fig. 9(c), we found that the target dose inhomogeneity was slightly improved.

## IV. CONCLUSIONS

The formalism we derived here provides a general starting point for the study of a system with a probability density-based dose prescription. The inclusion of the partial information into the plan selection process represents a significant change from the conventional approaches. The proposed technique can be categorized into the general Bayesian decision-making theory,[31] which is a useful tool to deal with a system with "statistical" inference. In image analysis and many other fields of science and engineering, it has proven extremely useful to include the prior knowledge of the system variables into the estimation process.[31] The preference function proposed for radiotherapy optimization here serves as *a priori* probability density function in standard Bayesian statistics. The role of the preference function is to indicate our "bias" on the values of the system variables. By utilizing the partial information of the system variables, one can more effectively search the solution space and eliminate some unnecessary uncertainties in the optimization process.

In conclusion, we have developed a statistical analysis-based inverse planning algorithm to include preference and expert knowledge into the dose optimization process. Instead of a rigid dose prescription, the new approach allows us to prescribe a range of doses with predesigned preference levels. The technique represents a novel application of the general Bayesian decision-making theory[31] for dealing with statistical inference and is valuable for deriving a statistically optimal solution in the presence of uncertainties in system parameters. The method was demonstrated for a system with modulating prescriptions but can be easily extended to solve many other related problems (e.g., in biologically based dose optimization, one can incorporate the uncertainties of various radiobiology parameters into the inverse planning process using the frameset developed in this work[35]). The ill conditioning of the problem was improved because of the use of a less restrictive prescription and, as a result, new solutions that are otherwise inaccessible can be obtained naturally. It is demonstrated that the obtained solutions using the new approach strongly correlate with the preference function, suggesting that the planning process is controllable and predictable by the proposed method.

[a] Author to whom correspondence should be addressed. Stanford University School of Medicine, Department of Radiation Oncology, 300 Pasteur Drive, Stanford, California 94305-5304. Electronic mail: lei@reyes.stanford.edu; phone: (650) 498 7896; fax: (650) 498 4015.

[1] T. Bortfeld, W. Schlegel, C. Dykstra, S. Levegrun, and K. Preiser, "Physical vs. biological objectives for treatment plan optimization," Radiother. Oncol. **40**, 185–187 (1996).

[2] T. Bortfeld, J. Stein, and K. Preiser. "Clinically relevant intensity modulation optimization using physical criteria," in *Proceedings of the XII International Conference on the Use of Computers in Radiation Therapy*, Salt Lake City, UT, 1997.

[3] L. Xing and G. T. Chen, "Iterative methods for inverse treatment planning," Phys. Med. Biol. **41**, 2107–2123 (1996).

[4] P. S. Cho, S. Lee, R. J. Marks II, S. Oh, S. G. Sutlief, and M. H. Phillips, "Optimization of intensity modulated beams with volume constraints using two methods: cost function minimization and projections onto convex sets," Med. Phys. **25**, 435–443 (1998).

[5] B. S. Teh, S. Y. Woo, and E. B. Butler, "Intensity modulated radiation therapy (IMRT): a new promising technology in radiation oncology," Oncologist **4**, 433–442 (1999).

[6] Y. Xiao, J. Galvin, M. Hossain, and R. Valicenti, "An optimized forward-planning technique for intensity modulated radiation therapy," Med. Phys. **27**, 2093–2099 (2000).

[7] S. M. Crooks and L. Xing, "Linear algebraic methods applied to intensity modulated radiation therapy," Phys. Med. Biol. **46**, 2587–2606 (2001).

[8] G. Starkschall, A. Pollack, and C. W. Stevens, "Treatment planning using a dose-volume feasibility search algorithm," Int. J. Radiat. Oncol., Biol., Phys. **49**, 1419–1427 (2001).

[9] A. Brahme, "Optimized radiation therapy based on radiobiological objectives," Semin Radiat. Oncol. **9**, 35–47 (1999).

[10] M. Langer, "Application of coloring theory to reduce intensity modulated radiotherapy dose calculations," Med. Phys. **27**, 2077–2083 (2000).

[11] I. C. W. Group, "Intensity-modulated radiotherapy: current status and issues of interest," Int. J. Radiat. Oncol., Biol., Phys. **51**, 880–914 (2001).

[12] G. A. Ezzell, "Genetic and geometric optimization of three-dimensional radiation therapy treatment planning," Med. Phys. **23**, 293–305 (1996).

[13] G. Starkschall, "A constrained least-squares optimization method for external beam radiation therapy treatment planning," Med. Phys. **11**, 659–665 (1984).

[14] D. H. Hristov and B. G. Fallone, "An active set algorithm for treatment planning optimization," Med. Phys. **24**, 1455–1464 (1997).

[15] C. B. Saw, K. M. Ayyangar, W. Zhen, M. Yoe-Sein, S. Pillai, and C. A. Enke, "Clinical implementation of intensity-modulated radiation therapy," Med. Dosim **27**, 161–169 (2002).

[16] K. S. Chao, F. J. Wippold, G. Ozyigit, B. N. Tran, and J. F. Dempsey, "Determination and delineation of nodal target volumes for head-and-neck cancer based on patterns of failure in patients receiving definitive and postoperative IMRT," Int. J. Radiat. Oncol., Biol., Phys. **53**, 1174–1184 (2002).

[17] S. Webb, "Optimisation of conformal radiotherapy dose distributions by simulated annealing," Phys. Med. Biol. **34**, 1349–1370 (1989).

[18] G. S. Mageras and R. Mohan, "Application of fast simulated annealing to optimization of conformal radiation treatments," Med. Phys. **20**, 639–647 (1993).

[19] X. H. Wang, R. Mohan, A. Jackson, S. A. Leibel, Z. Fuks, and C. C. Ling, "Optimization of intensity-modulated 3D conformal treatment plans based on biological indices," Radiother. Oncol. **37**, 140–152 (1995).

[20] L. Jones and P. Hoban, "A method for physically based radiotherapy

optimization with intelligent tissue weight determination," Med. Phys. **29**, 26–37 (2002).

[21] R. P. Li and F. F. Yin, "Optimization of inverse treatment planning using a fuzzy weight function," Med. Phys. **27**, 691–700 (2000).

[22] Y. Chen, D. Michalski, C. Houser, and J. M. Galvin, "A deterministic iterative least-squares algorithm for beam weight optimization in conformal radiotherapy," Phys. Med. Biol. **47**, 1647–1658 (2002).

[23] L. Xing, J. G. Li, S. Donaldson, Q. T. Le, and A. L. Boyer, "Optimization of importance factors in inverse planning," Phys. Med. Biol. **44**, 2525–2536 (1999).

[24] X. Wu and Y. Zhu, "An optimization method for importance factors and beam weights based on genetic algorithms for radiotherapy treatment planning," Phys. Med. Biol. **46**, 1085–1099 (2001).

[25] C. Cotrutz and L. Xing, "Using voxel-dependent importance factors for interactive DVH-based dose optimization," Phys. Med. Biol. **47**, 1659–1669 (2002).

[26] S. V. Spirou and C. S. Chui, "A gradient inverse planning algorithm with dose-volume constraints," Med. Phys. **25**, 321–333 (1998).

[27] A. Niemierko, M. Urie, and M. Goitein, "Optimization of 3D radiation therapy with both physical and biological end points and constraints," Int. J. Radiat. Oncol., Biol., Phys. **23**, 99–108 (1992).

[28] C. De Wagter, C. O. Colle, L. G. Fortan, B. B. Van Duyse, D. L. Van den Berge, and W. J. De Neve, "3D conformal intensity-modulated radiotherapy planning: interactive optimization by constrained matrix inversion," Radiother. Oncol. **47**, 69–76 (1998).

[29] S. M. Morrill, R. G. Lane, J. A. Wong, and I. I. Rosen, "Dose-volume considerations with linear programming optimization." Med. Phys. **18**, 1201–10 (1991).

[30] S. M. Morrill, K. S. Lam, R. G. Lane, M. Langer, and I. I. Rosen, "Very fast simulated reannealing in radiation therapy treatment plan optimization," Int. J. Radiat. Oncol., Biol., Phys. **31**, 179–188 (1995).

[31] L. Xing, J. G. Li, A. Pugachev, Q. T. Le, and A. L. Boyer, "Estimation theory and model parameter selection for therapeutic treatment plan optimization," Med. Phys. **26**, 2348–2358 (1999).

[32] Q. Wu and R. Mohan, "Algorithms and functionality of an intensity modulated radiotherapy optimization system," Med. Phys. **27**, 701–711 (2000).

[33] C. Cotrutz, M. Lahanas, C. Kappas, and D. Baltas, "A multiobjective gradient-based dose optimization algorithm for external beam conformal radiotherapy," Phys. Med. Biol. **46**, 2161–2175 (2001).

[34] J. Llacer, "Inverse radiation treatment planning using the Dynamically Penalized Likelihood method," Med. Phys. **24**, 1751–1764 (1997).

[35] L. Xing, J. Lian, and C. Cotrutz, "Inverse treatment planning with inclusion of model parameter uncertainty," in the 44th Annual AAPM Meeting, Montreal, 2002.

[36] R. B. Altman and R. Tombropoulos, "Probabilistic constraint satisfaction: application to radiosurgery," in the 18th Annual Symposium on Computer Applications in Medical Care, Washington, DC, 1994.

# Incorporating Model Parameter Uncertainty into Inverse

# Treatment Planning

Jun Lian and Lei Xing[a]


Department of Radiation Oncology, Stanford University School of Medicine,

300 Pasteur Drive, Stanford, California, CA 94305-5304


a) Author to whom correspondence should be addressed.

Stanford University School of Medicine
Department of Radiation Oncology
875 Blake Wilbur Drive
Stanford, CA 94305-5847

E-mail: lei@reyes.stanford.edu
Phone: (650) 498 7896
Fax:    (650) 498 4015

1

# ABSTRACT

Radiobiological treatment planning depends not only on the accuracy of the models describing the dose-response relation of different tumors and normal tissues but also on the accuracy of tissue specific radiobiological parameters in these models. Whereas the general formalism remains the same, different sets of model parameters lead to different solutions and thus critically determine the final plan. Here we describe an inverse planning formalism with inclusion of model parameter uncertainties. This is made possible by using a statistical analysis-based frameset developed by our group. In this formalism, the uncertainties of model parameters, such as the parameter $a$ that describes tissue-specific effect in EUD model, are expressed by probability density function and are included in the dose optimization process. We found that the final solution strongly depends on distribution functions of the model parameters. Considering that currently available models for computing biological effects of radiation are simplistic, and the clinical data used to derive the models are sparse and of questionable quality, the proposed technique provides us with an effective tool to minimize the effect caused by the uncertainties in a statistical sense. With the incorporation of the uncertainties, the technique has potential for us to maximally utilize the available radiobiology knowledge for better IMRT treatment.


Key words: inverse planning, dose optimization, biological models, IMRT

# INTRODUCTION

Most IMRT optimization systems at present use dose and/or dose volume-based objective functions [1-6], which guide the IMRT planning by imposing a penalty according to the difference between the computed and prescribed doses. A well-known drawback of the dose-based inverse planning is that the nonlinear dose response of tumor or normal structures is not fully considered. A number of mathematical models have been developed over the years to better describe the biological effect of radiation, which include tumor control probability (TCP) [7], normal tissue complication probability (NTCP) [8], equivalent uniform dose (EUD) [9] and the probability of uncomplicated tumor control ($P_+$) [10, 11]. In parallel to these modeling efforts, considerable works have also been done to use these biological models to construct more meaningful objective functions for therapeutic dose optimization [11-16].

Generally speaking, radiobiological formalism involves the use of model parameters that are of considerable uncertainty [7, 17-22]. For instance, the radiosensitivity $\alpha$ of Webb's TCP model varies from 0.157 Gy$^{-1}$ to 0.090 Gy$^{-1}$ when model parameters were fit to 103 patients' data [7]. Biological 'margins' have been used to account for the variability in radiation sensitivity. Similar to the use of a safety margin to account for the potential uncertainties in targeting a tumor, this method assigns more conservative radiosensitivity values to the tumor or sensitive structures to deal with the potential uncertainty of the parameter[23]. Kåver et al proposed a stochastic optimization to account for clinical uncertainties, including the varying radiosensitivity [24, 25]. The objective function was constructed based on a linear quadratic Poisson model which approximates the probability of curing the patient or inflicting injury. Two parameters in the model

could be calculated if the standard deviation of dose per faction was known. The optimization was thus executed corresponding to different standard deviations.

We have recently presented a general statistical analysis-based inverse planning framework [26, 27] and applied it to investigate the influence of model parameter uncertainties in biologically based dose optimization [28]. The purpose of this paper is to provide a detailed description of the technique and addresses several important issues related to the dose optimization in the presence of model parameter uncertainties. In our approach, the uncertainty of a model parameter is quantified by a probability density function and its influence is then incorporated into inverse planning through the use of a statistical inference theorem [26]. The technique is illustrated by using a hypothetical C-shaped tumor case, a prostate tumor case and a paraspinal tumor case with an EUD-based model. Considering that currently available models for computing biological effects of radiation are simplistic, and the data they rely on are sparse and of questionable quality, the proposed technique provides us with an effective tool to minimize the effect caused by the uncertainties in a statistical sense. The treatment plans so obtained are generally less sensitive to the inter-patient variation and other types of uncertainties that may otherwise influence the final treatment plan greatly.

# METHODS AND MATERIALS

## Statistical analysis-based inverse planning

The inverse problem as posed for IMRT consists of the determination of the beamlet weight vector $w$ when a desired plan is prescribed. In a vectorial form, the dose to the points in the treatment region depends upon the beamlet weights $w$ as

$$D_c = d \cdot w, \qquad (1)$$

where $d$ represents the dose deposition coefficients matrix, expressing the dose deposited to any patient point when irradiated with a unit weight beamlet. The total number of physically realizable dose distributions $D_c$ in IMRT is enormous and increases exponentially with the number of beamlets. Inverse planning is essentially a plan selection process from the vast pool of physically realizable solutions. In a recent paper, Xing et al [26] introduced a statistical analysis-based inverse planning technique. In this approach the commonly used objective function is reformulated into a probability density function whose value gives the figure of merit of a dose distribution. A virtue of the approach is that it allows us to obtain solution in the presence of uncertainties of the prescription parameters or other model parameters using a statistical inference technique. Application of the technique to deal with a system with a set of variable dose prescriptions has been described in another work of our group [27]. Here we use the formalism for biological modeling based- inverse planning in the presence of model parameter uncertainties. To be specific, we use an equivalent uniform dose (EUD)-based objective function employed by Wu et al [13, 29] and discuss the consequences of the variation of model parameter $a$ and how to incorporate the fluctuations into inverse planning dose optimization to obtain statistically optimal solutions.

## EUD model and EUD-based objective function

The concept of equivalent uniform dose (EUD) for tumor was originally introduced by Niemierko as the biologically equivalent dose that, if given uniformly, would lead to the same cell kill in the tumor volume as the actual nonuniform dose distribution. Recently, Niemierko et al suggested a phenomenological form [9, 13, 30]:

$$EUD = \left( \frac{1}{N} \sum_i D_i^{a} \right)^{\frac{1}{a}} \tag{2}$$

for both tumor and normal tissues, where $N$ is the number of voxels in the structure, $D_i$ is the dose delivered to the $i$th voxel, $a$ is the tumor or normal tissue-specific parameter that describes the dose-volume effect. EUD described in Eq. (2) is the general mean of the non-uniform dose distribution. According to the mathematic properties of the function [31], for $a = \infty$, the EUD is equal to the maximum dose, and for $a = -\infty$, the EUD is equal to the minimum dose. Tumors generally have large negative values of $a$, whereas serial critical structures (e.g. spinal cord and rectum) have large positive values and parallel critical structures that exhibit a large dose-volume effect (e.g. liver, parotids, and lungs) have small positive values.

The objective function or figure of merit used to measure the goodness of a dose distribution and guide the optimization [1]. In the present paper, the system objective function is given by [13]

$$F = \prod_j f_j, \tag{3}$$

where the component subcore $f_j$ may be either

$$f_T = \frac{1}{1 + \left(\dfrac{EUD_0}{EUD}\right)^n} \tag{4}$$

for tumors, or

$$f_{OAR} = \frac{1}{1 + \left(\dfrac{EUD}{EUD_0}\right)^n} \tag{5}$$

for normal tissues and organs at risk (OARs). $EUD_0$ is the desired dose parameter for the target volume and the maximum tolerable uniform dose for normal structures. Parameter $n$ is akin to the structure specific importance factor [32] in the conventional inverse planning formalism that parameterizes our tradeoff strategy of different structure. The large $n$ indicates high importance.

**Incorporation of the variation distribution of the model parameter into inverse planning**

We assume that $a_k$ in the EUD model varies according to a simple Gaussian distribution

$$P_n(a_k) = P'_{o_n} \exp\{-r_n[a_k - a_o]^2\}, \tag{6}$$

where $a_0$ is the mean value, $P'_{o_n}$ is a normalization constant and $a_k$ is one of the sampling values of $a$. For a given distribution, the EUD and the corresponding figure of merit of an IMRT plan vary with the sampling of $a$. We thus rewrite Eqs. (4) and (5) as conditional probabilities for a sampled $a_k$:

$$P_T(EUD \mid a_k) = \frac{1}{1+\left(\dfrac{EUD_0}{EUD}\right)^n}, \tag{7}$$

$$P_{OAR}(EUD \mid a_k) = \frac{1}{1+\left(\dfrac{EUD}{EUD_0}\right)^n}. \tag{8}$$

The objective function for a structure $m$ in the presence of uncertainty in $a$ is expressed as the summation of a series of joint probabilities

$$P_m(EUD) = \sum_k P_m(EUD \mid a_k) \cdot P_m(a_k), \tag{9}$$

and the overall objective function $P$ of the system is a product of $P_m(EUD)$ defined in Eq. (9). That is

$$F = \ln(1/P) = -\ln \prod_m P_m(EUD) = -\sum_m \ln \sum_k P_m(EUD \mid a_k) \cdot P_m(a_k). \tag{10}$$

**Optimization method**

As described above, the uncertainties of model parameters, $\{a_k\}$, are described by probability density functions and they are incorporated into the overall objective function of the system through the joint probability given by Eq. (9). To obtain the optimal solution in the presence of model parameters, all we need to do is to minimize the overall objective function given by Eq. (10).

The calculation process is schematically shown in Fig. 1. For the computational purpose, the probability density function for each structure is discreted into seven equally spaced points. We use the Fletcher-Reeves conjugate gradient optimization algorithm [33] to optimize the system. But any other iterative or stochastic optimization can be also employed to optimize the system. A common step in all optimization algorithms is the

evaluation of the objective function for a trial beam profiles (or computed dose distribution), which is somewhat tedious here because of the appearance of multiple $a_k$'s of the involved structures. Briefly, for a given trial beam profiles or dose distribution, the evaluation of the objective function consists of four steps: (i) for a structure $m$, calculate the EUD corresponding to each possible $a_k$; (ii) calculate the conditional probability for the target and OAR using Eq. (7) and (8), respectively; (iii) sum over all possible $a_k$ to obtain the joint probability, given by Eq. (9); and (iv) sum over all structures to obtain the overall objective function value. After the dose optimization, a set of optimal beam profiles and the corresponding dose distribution and other plan indices are provided for the planner to assess the clinical relevance of the obtained treatment plan.

**Test cases**

The new algorithm was tested using a hypothetical phantom case with a C-shaped target and two clinical cases (a prostate case and a paraspinal tumor boost treatment). The size of the pencil beam defined at the isocenter was 0.5 cm. The configuration of the C-shaped tumor case is shown in Fig. 2A. Nine 6MV equi-spaced beams were used for the treatment (0°, 40°, 80°, 120°, 160°, 200°, 240°, 280°, and 320° – respecting the IEC convention). The values of $n$ and $a$ in the EUD-based objective function are listed in Table 1. The parameter $a$ in EUD model characterizes the dose-volume effect but its value is generally not known accurately even for clinically well studied organs. The influence of the uncertainty in the $a$ value of a target or sensitive structure to the final treatment plan was studied and analyzed.

Similar study was carried out for the two clinical cases. The six 6MV beam angles used for the IMRT prostate treatment were 0°, 55°, 135°, 180°, 225° and 305°. Table 2

lists some relevant parameters used for planning the case. For the IMRT paraspinal boost treatment, five 6 MV non-equally spaced coplanar beams were placed at the following angular positions: 95°, 140°, 175°, 225° and 275°. The target boost dose was prescribed to 16 Gy. Relevant parameters are listed in Table 2. The planning goal was to find a dose distribution that covered the tumor volume as uniformly as possible, while maximally sparing the spinal cord, liver, and kidney.

# RESULTS AND DISCUSSIONS

## The C-shaped tumor case

We first investigated the behavior of the system when the parameter $a$ of the target EUD takes four different distributions, as depicted in the bar charts shown on the right of Fig. 3, while keeping the parameter $a$ of the OAR at a constant $a_0 = 6.0$. In the case shown in Fig. 3 d1, the parameter $a$ takes only a single value, $a_0 = -10$, which is a simple case studied by Wu et al [13]. The optimal plans for the four distributions of parameter $a$ differ significantly, as indicated by the target and OAR DVHs shown in Fig. 3 A and B. The isodose plot corresponding to the $a$-distribution shown in Fig. 3 d2 is plotted in Fig. 2B.

To estimate the degree of sensitivity of the solutions against a variation in $a$, we computed the target EUD and the objective function, $f_T$, as a function of parameter $a$ for the four optimal dose distributions under different types of uncertainty distributions. The

results are plotted in Fig. 4. For plan A, the EUD changes from 65 to 71 Gy when $a$ is varied from $-10$ to $-70$ and to 79 Gy when $a$ is equal to 140. The objective function varies from 0.11 to 0.85 in the range of variation in $a$. For plan D, the EUD is narrowed to a range between 70 Gy and 79 Gy. The EUD variations of plans B and C are similarly reduced. These results suggest that the EUD becomes much less sensitive to the variation in parameter $a$ in the plans obtained with some "built-in" distributions in parameter $a$ (i.e., plans corresponding to Figs. 3 d2 to d4).

The uncertainty of parameter $a$ of the OAR can be similarly included in the dose optimization process when its distribution is known. In the second study, we fixed the target EUD parameter $a = -10$ and allowed the parameter $a$ of the OAR to take four different distributions as plotted in the right of Fig. 5. The target and OAR DVHs for the four possible scenarios are shown in A and B. Once again, we found that the final solution strongly depends on the distributions of the parameter $a$.

The maximum doses of the OAR of the four plans vary from 24 Gy to 30 Gy. Note that the doses to the OAR in plans B, C and D are less than that of plan A, where the parameter $a$ is restricted to a single value, $a_0 = 6$. This is explainable since the parameters $a$ in plans d2, d3 and d4 are shifted up to higher values. As $a$ increases, the EUD puts more emphasis on the high dose (recall that EUD becomes the maximum dose when $a = \infty$). As a consequence of the increased "effective" $a$ value in the distributions shown in Figs. 5 d2, d3 and d4, the OAR dose is improved in comparison with the plan obtained under the assumption of a fixed $a$ value (Fig. 5 d1). Interestingly, the target DVHs shows that four distinct plans have very similar target coverage. It is well known that in dose optimization there is generally no net gain: an improvement in the dose to a structure is

often accompanied by a dosimetrically adverse effect(s) at other points in the same or different structures. The result here suggests that, from a clinical point of view, it is possible to have a great gain in one structure with a little sacrifice in another structure. How to find the truly optimal tradeoff represents a practical subject that is worth of studying in the future.

As can be expected from the discussion in previous paragraphs, the solution obtained with $a_0 = 6$ (Fig. 5 d1) is more sensitive to a variation in parameter $a$. Indeed, as seen from Fig. 6, the EUD for this plan varies from 1 Gy to 30 Gy when $a$ is changed from -80 to 140. On the other hand, the EUD changes for the rest three situations are much less for the same variation in $a$. The upper bound of the EUD is reduced to 26 Gy for plan d4, 24 Gy for plan d2, and 23 Gy for plan d3. The objective functions of four plans show a similar trend.

**The prostate tumor case**

Four IMRT plans with different types of pre-assumed uncertainties were generated for a prostate tumor case (Fig. 7A). These include: (i) The $a$-parameters for both prostate target and OARs are restricted to single values as listed in Table 2. This plan serves as a reference whose DVHs are shown in Figs. 8A-8C as dotted curves; (ii) Only the $a$-parameter of the prostate target takes a range of values, as depicted in the right of Fig. 8A; (iii) Only the $a$-parameter of the rectum takes a range of values, as depicted in the right of Fig. 8B; and (iv) The $a$-parameters of both prostate target and the rectum were allowed to take a range of values, as depicted in the right of Fig. 8C.

DVHs for the plan using parameters defined in Table 2 are plotted with dotted curves and plans with the inclusion of parameter uncertainty are drawn with solid curves (Fig. 8). When the parameter $a$ in target EUD takes a Poisson distribution as shown in the bar chart of Fig. 8A, prostate dose homogeneity is significantly improved. The minimum dose increases from 55 Gy to 67 Gy, and the maxim dose decreases slightly from 82 Gy to 80Gy. However the volumes receiving radiation dose for rectum, bladder and normal tissue all increase significantly though the maximum dose remains similar. The improvement of the target coverage and compromise of OAR sparing is a natural outcome of the competitive requirements for targets and OARs imposed on the system. The corresponding dose distribution with the target parameter defined in the bar chart A is shown in Fig. 7B.

Next we considered the inclusion of parameter $a$ uncertainty in EUD calculation in one of the critical structures-rectum (Fig. 8 B). The irradiated rectum volume for a dose below 60 Gy is less than that of a conventional plan with the parameter $a$ fixed at 24. DVHs for the bladder, normal tissue and prostate do not change significantly compared to the plan without inclusion of parameter uncertainty.

Lastly, we simultaneously replaced target and rectum parameters with the distributions shown in Fig. 8 C. Similar to that corresponds the prescription of Fig. 8 A, the prostate coverage is improved. However, the rectum DVH in this case is not worsen greatly because parameter $a$ of rectum EUD was allowed to take a spectrum of values. For bladder and normal tissue, although their irradiated volumes in the low dose region are higher than those of the conventional plan, the volumes receiving high doses are reduced.

**The paraspinal tumor case**

Three IMRT plans were generated for a paraspinal tumor case (Fig. 9A). These include: (i) The $a$-parameters for both prostate target and OARs are restricted to single values as listed in Table 3. This plan serves as a reference whose DVHs are shown in Figs. 9B-C as dotted curves; (ii) Only the $a$-parameter of the target takes a range of values, as depicted in the right of Fig. 9B; and (iii) Only the $a$-parameter of the spinal cord takes a range of values, as depicted in the right of Fig. 9C.

When $a$ in target EUD takes a Poisson distribution as shown in the bar chart of Fig. 9B, dose homogeneity is slightly improved. However this is achieved at the expense of more irradiation to the cord. The inclusion of parameter $a$ uncertainty in EUD calculation in the spinal cord (Fig. 9C) reduced the maximum cord dose by 100 cGy. The DVHs of the target, kidney, and liver were not changed significantly compared to the plan without inclusion of parameter uncertainty.

The influence of various uncertainties on the patient treatment has been a subject of intense study. Fenwick and Nahum have included the model parameter uncertainty with a standard deviation when calculating the NTCP of rectum [34, 35]. Similarly, the inclusion of uncertainties in the patient setup and dose calculation has also been demonstrated [36-38]. Deasy et al have used a bootstrap-based method to estimate the influence of biological parameter uncertainties on predicting long-term salivary function [38]. The statistical method proposed here provides a general framework to include various uncertainties in the dose optimization process. With minor modification, the technique

can be extended to derive statistically optimal solutions in the presence of other types of uncertainties.

As can be intuitively imagined, the inclusion of $a$-distribution will definitely change the final dose. Whether it will improve or worsen the final dose distribution will generally depend on the specific form of the $a$-distribution, and also the metric used to judge the goodness of a plan. If the original EUD-based objective function is used as the sole metric for the judgment, the inclusion of $a$-distribution may make the plan worse. However, clinical decision-making is not made by a single function and a "worse" plan judged by the EUD-objective function may turn out to be clinically more favorable. In other words, there is a gap between mathematical dose optimization and clinical decision-making. The study seems to suggest that, while it is generally true that there is no net gain in dose optimization [27], it is important to develop a method that is capable of optimizing not only the objective function but also the next level of decision-making. This kind of optimization will allow us to find the solution that may sacrifice a little (i.e., clinically insignificant) in one or a few structures but gain a lot in other structures.

## CONCLUSIONS

We have proposed and implemented a technique for incorporating biological model parameter uncertainties into inverse treatment planning. The formalism is quite general and does not prerequisite the specific form of uncertainty distributions of the involved model parameters. By including model parameter uncertainties, the final solution becomes more robust and the treatment outcome will be less likely influenced by inter-patient variation of biological characteristics. With the increasing interest in

radiation therapy community to use biologically based models for treatment planning, this work provides an effective way to better account for the known uncertainties in the model parameters and allows us to maximally utilize the available radiobiology knowledge to facilitate patient care.

## ACKNOWLEDGEMENTS

# REFERENCE

1    Q. Wu and R. Mohan, Algorithms and functionality of an intensity modulated radiotherapy optimization system. Med Phys. 27, 701-11 (2000).

2    G. Starkschall, A. Pollack, and C.W. Stevens, Treatment planning using a dose-volume feasibility search algorithm. Int J Radiat Oncol Biol Phys. 49, 1419-27 (2001).

3    L. Xing, R.J. Hamilton, D. Spelbring, C.A. Pelizzari, G.T. Chen, and A.L. Boyer, Fast iterative algorithms for three-dimensional inverse treatment planning. Med Phys. 25, 1845-9. (1998).

4    P.S. Cho, S. Lee, R.J. Marks, 2nd, S. Oh, S.G. Sutlief, and M.H. Phillips, Optimization of intensity modulated beams with volume constraints using two methods: cost function minimization and projections onto convex sets. Med Phys. 25, 435-43 (1998).

5    T. Bortfeld, Optimized planning using physical objectives and constraints. Semin Radiat Oncol. 9, 20-34. (1999).

6    S. Webb, Optimisation of conformal radiotherapy dose distributions by simulated annealing. Phys Med Biol. 34, 1349-70 (1989).

7    S. Levegrun, A. Jackson, M.J. Zelefsky, M.W. Skwarchuk, E.S. Venkatraman, W. Schlegel, Z. Fuks, S.A. Leibel, and C.C. Ling, Fitting tumor control probability models to biopsy outcome after three-dimensional conformal radiation therapy of prostate cancer: pitfalls in deducing radiobiologic parameters for tumors from clinical data. Int J Radiat Oncol Biol Phys. 51, 1064-80 (2001).

8    J.T. Lyman, Complication probability as assessed from dose-volume histograms. Radiat Res Suppl. 8, S13-9 (1985).

9    A. Niemierko, Reporting and analyzing dose distributions: a concept of equivalent uniform dose. Med Phys. 24, 103-10 (1997).

10   G.O. De Meerleer, L.A. Vakaet, W.R. De Gersem, C. De Wagter, B. De Naeyer, and W. De Neve, Radiotherapy of prostate cancer with or without intensity modulated beams: a planning comparison. Int J Radiat Oncol Biol Phys. 47, 639-48. (2000).

11   C. Fiorino, S. Broggi, D. Corletto, G.M. Cattaneo, and R. Calandrino, Conformal irradiation of concave-shaped PTVs in the treatment of prostate cancer by simple 1D intensity-modulated beams. Radiother Oncol. 55, 49-58. (2000).

12    M. Alber and F. Nusslin, An objective function for radiation treatment optimization based on local biological measures. Phys Med Biol. 44, 479-93 (1999).

13    Q. Wu, R. Mohan, A. Niemierko, and R. Schmidt-Ullrich, Optimization of intensity-modulated radiotherapy plans based on the equivalent uniform dose. Int J Radiat Oncol Biol Phys. 52, 224-35 (2002).

14    A. Brahme, J. Nilsson, and D. Belkic, Biologically optimized radiation therapy. Acta Oncol. 40, 725-34 (2001).

15    X.H. Wang, R. Mohan, A. Jackson, S.A. Leibel, Z. Fuks, and C.C. Ling, Optimization of intensity-modulated 3D conformal treatment plans based on biological indices. Radiother Oncol. 37, 140-52 (1995).

16    C. Thieke, T. Bortfeld, A. Niemierko, and S. Nill, From physical dose constraints to equivalent uniform dose constraints in inverse radiotherapy planning. Med Phys. 30, 2332-9 (2003).

17    C. Burman, G.J. Kutcher, B. Emami, and M. Goitein, Fitting of normal tissue tolerance data to an analytic function. Int J Radiat Oncol Biol Phys. 21, 123-35 (1991).

18    S. Webb and A.E. Nahum, A model for calculating tumour control probability in radiotherapy including the effects of inhomogeneous distributions of dose and clonogenic cell density. Phys Med Biol. 38, 653-66 (1993).

19    P.M. Wu, D.T. Chua, J.S. Sham, L. Leung, D.L. Kwong, M. Lo, A. Yung, and D.T. Choy, Tumor control probability of nasopharyngeal carcinoma: a comparison of different mathematical models. Int J Radiat Oncol Biol Phys. 37, 913-20 (1997).

20    J.D. Fenwick, Predicting the radiation control probability of heterogeneous tumour ensembles: data analysis and parameter estimation using a closed-form expression. Phys Med Biol. 43, 2159-78 (1998).

21    J.O. Deasy, K.S. Chao, and J. Markman, Uncertainties in model-based outcome predictions for treatment planning. Int J Radiat Oncol Biol Phys. 51, 1389-99 (2001).

22    R. Jeraj and P. Keall, The effect of statistical uncertainty on inverse treatment planning based on Monte Carlo dose calculation. Phys Med Biol. 45, 3601-13. (2000).

23    A. Brahme, Optimized radiation therapy based on radiobiological objectives. Semin Radiat Oncol. 9, 35-47 (1999).

24    G. Kåver, B.K. Lind, J. Lof, A. Liander, and A. Brahme, Stochastic optimization of intensity modulated radiotherapy to account for uncertainties in patient sensitivity. Phys Med Biol. 44, 2955-69 (1999).

25    J. Lof, B.K. Lind, and A. Brahme, An adaptive control algorithm for optimization of intensity modulated radiotherapy considering uncertainties in beam profiles, patient set-up and internal organ motion. Phys Med Biol. 43, 1605-28 (1998).

26    L. Xing, J.G. Li, A. Pugachev, Q.T. Le, and A.L. Boyer, Estimation theory and model parameter selection for therapeutic treatment plan optimization. Med Phys. 26, 2348-58 (1999).

27    J. Lian, C. Cotrutz, and L. Xing, Therapeutic treatment plan optimization with probability density-based dose prescription. Med Phys. 30, 655-66 (2003).

28    L. Xing, J. Lian, and C. Cotrutz. *Inverse treatment planning with inclusion of model parameter uncertainty.* in *the 44th Annual AAPM Meeting.* Montreal(2002).

29    B. Choi and J.O. Deasy, The generalized equivalent uniform dose function as a basis for intensity-modulated treatment planning. Phys Med Biol. 47, 3579-89 (2002).

30    P. Mavroidis, B.K. Lind, and A. Brahme, Biologically effective uniform dose (D) for specification, report and comparison of dose response relations and treatment plans. Phys Med Biol. 46, 2607-30 (2001).

31    M. Abramowitz and I.A. Stegun, *Handbook of mathematical functions with formulas, graphs, and mathematical tables*, Wiley-Interscience: New York. p. 1046 (1984).

32    L. Xing, J.G. Li, S. Donaldson, Q.T. Le, and A.L. Boyer, Optimization of importance factors in inverse planning. Phys Med Biol. 44, 2525-36 (1999).

33    C. Cotrutz, M. Lahanas, C. Kappas, and D. Baltas, A multiobjective gradient-based dose optimization algorithm for external beam conformal radiotherapy. Phys Med Biol. 46, 2161-75 (2001).

34    J.D. Fenwick, Impact of dose-distribution uncertainties on rectal ntcp modeling. II: Uncertainty implications. Med Phys. 28, 570-81 (2001).

35    J.D. Fenwick and A.E. Nahum, Impact of dose-distribution uncertainties on rectal ntcp modeling. I: Uncertainty estimates. Med Phys. 28, 560-9 (2001).

36    A.E. Lujan, E.W. Larsen, J.M. Balter, and R.K. Ten Haken, A method for incorporating organ motion due to breathing into 3D dose calculations. Med Phys. 26, 715-20 (1999).

37    P.J. Keall, J.V. Siebers, R. Jeraj, and R. Mohan, The effect of dose calculation uncertainty on the evaluation of radiotherapy plans. Med Phys. 27, 478-84 (2000).

38    J.G. Li and L. Xing, Inverse planning incorporating organ motion. Med Phys. 27, 1573-8. (2000).

# FIGURE CAPTIONS

Figure 1. The flow chart of the optimization process with the inclusion of model parameter uncertainty.

Figure 2. (A) The sketch of the hypothetical case with C-shaped target and the beam set-up for dose optimization. (B) The dose distribution corresponding to the parameters listed in Tab.1 and the probabilistic distribution shown in Fig. 3B.

Figure 3. The target and OAR DVHs of four optimal plans when parameter $a$ is a fixed value (bar chart d1) and varies according to three different probabilistic distributions (bar chart d2, d3 and d4).

Figure 4. The EUD of the target and objective function when parameter $a$ is prescribed according to Fig. 3.

Figure 5. The target and OAR DVHs of four optimal plans when parameter $a$ is a fixed value (bar chart d1) and varies according to three different probabilistic distributions (bar chart d2, d3 and d4).

Figure 6. The EUD of the OAR and objective function when parameter $a$ is prescribed according to Fig. 5.

Figure 7. A transverse slice showing the anatomical structures delineated for the prostate tumor (A) and the corresponding optimized dose distribution with the parameters listed in Tab. 2 and the probabilistic distribution shown in Fig. 8B.

Figure 8. DVHs for a prostate cancer case using the conventional optimization with fixed $a$-value (dotted line) and the newly proposed approach with the inclusion of model parameter uncertainty (solid line). (A) Only the $a$-parameter for the target is assigned with a probabilistic distribution; (B) Only the $a$-parameter for the OAR is assigned with a probabilistic distribution; (C) Uncertainties in the $a$-parameter are introduced for both the target and OAR.

Figure 9. (A) A transverse slice showing the anatomical structures for a paraspinal case; (B) DVHs when the $a$-parameter for the target is assigned with a probabilistic distribution; (C) DVHs when the $a$-parameter for the OAR is assigned with a probabilistic distribution.

Table 1. The conventional EUD-based optimization parameter for the hypothetical IMRT treatment of a C-shaped tumor.

|  | PTV | PTV* | OAR | NT |
|---|---|---|---|---|
| a | -10.0 | 10.0 | 6.0 | 6.0 |
| $EUD_0(Gy)$ | 72 | 76 | 35 | 35 |
| n | 20 | 20 | 6 | 6 |

* Contains parameters for the target treated as virtual normal tissue to limit dose inhomogeniety.

Table 2. The conventional EUD-based optimization parameter for prostate cancer.

|  | PTV | PTV* | Bladder | Rectum | NT |
|---|---|---|---|---|---|
| a | -10.0 | 10.0 | 6.0 | 24 | 6.0 |
| $EUD_0(Gy)$ | 72 | 76 | 35 | 35 | 35 |
| n | 20 | 20 | 6 | 6 | 6 |

* Contains parameters for the target treated as virtual normal tissue to limit dose inhomogeniety.

Table 3. The conventional EUD-based optimization parameter for paraspinal tumor.

|  | PTV | PTV* | Spine | Liver | Kidney |
|---|---|---|---|---|---|
| a | -10.0 | 10.0 | 6.0 | 6.0 | 6.0 |
| $EUD_0(Gy)$ | 16 | 17 | 12 | 6.4 | 4.8 |
| n | 20 | 20 | 6 | 6 | 6 |

* Contains parameters for the target treated as virtual normal tissue to limit dose inhomogeniety.
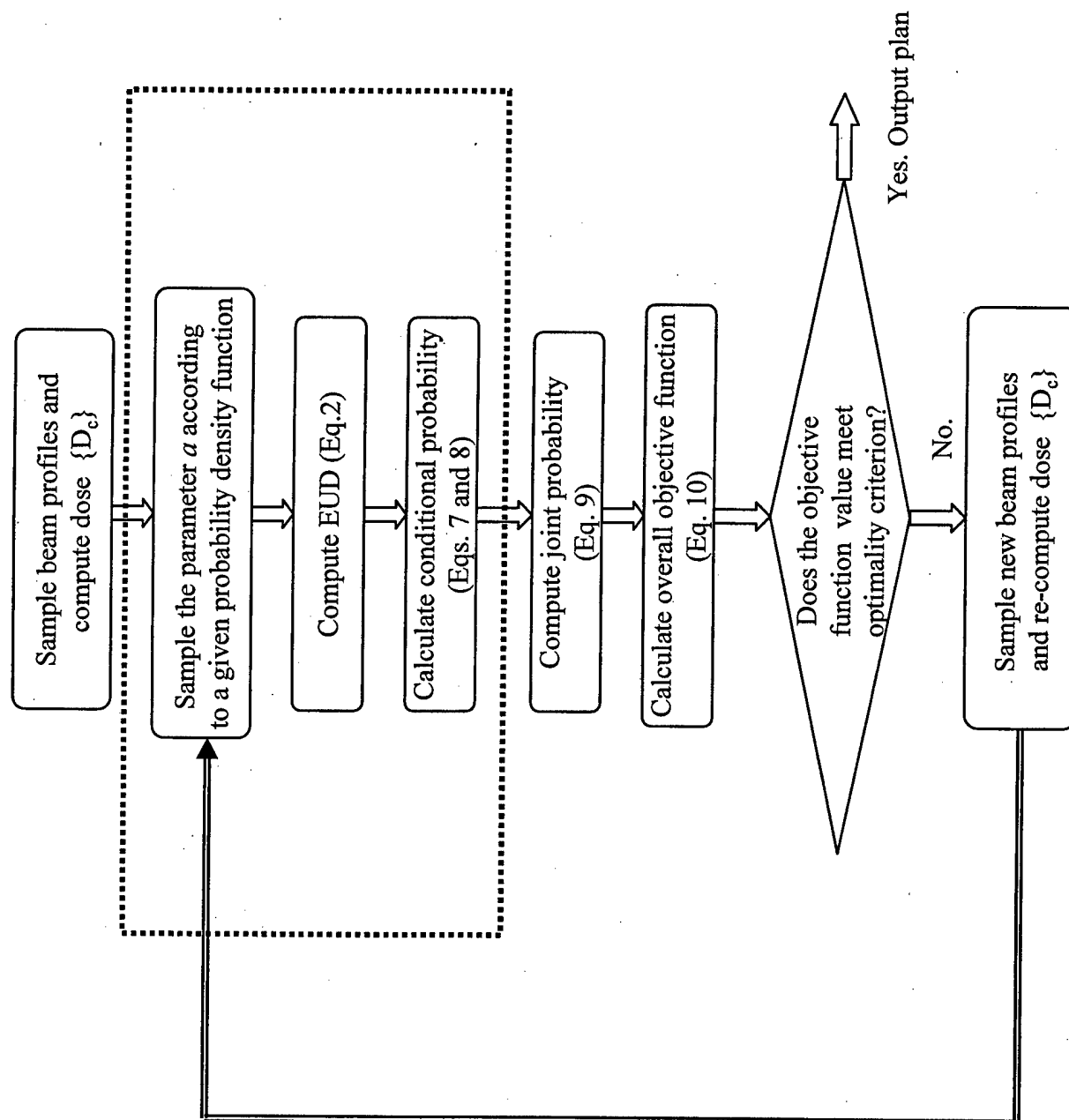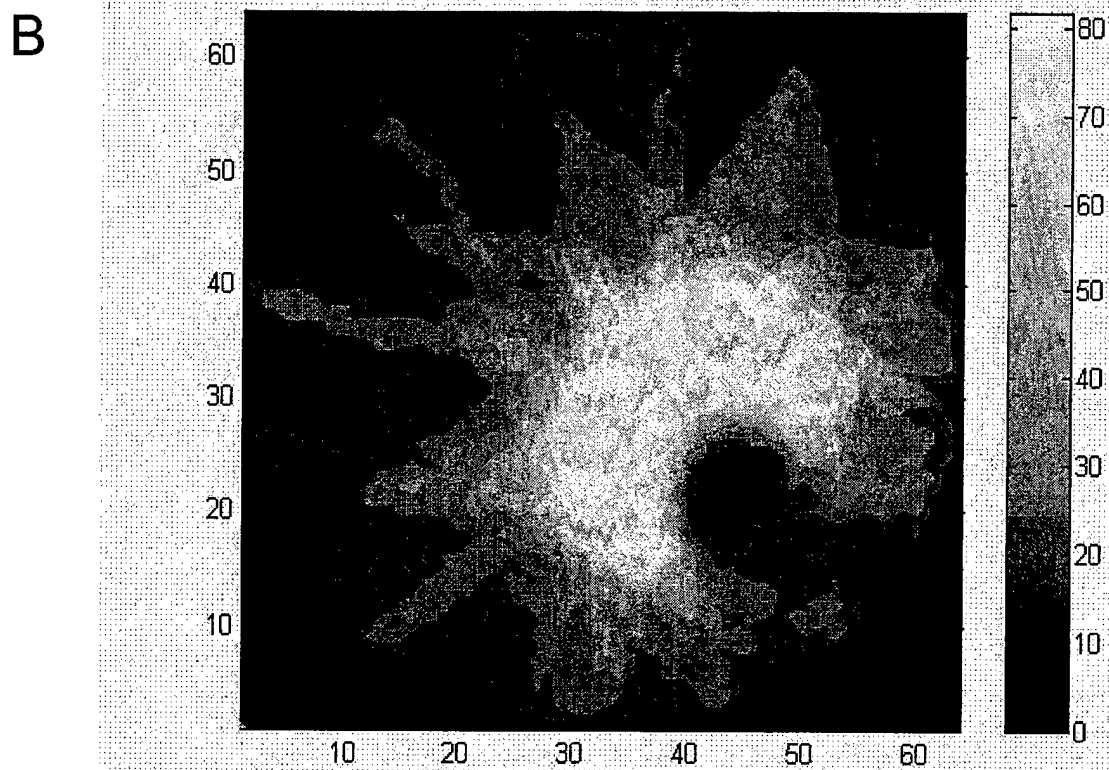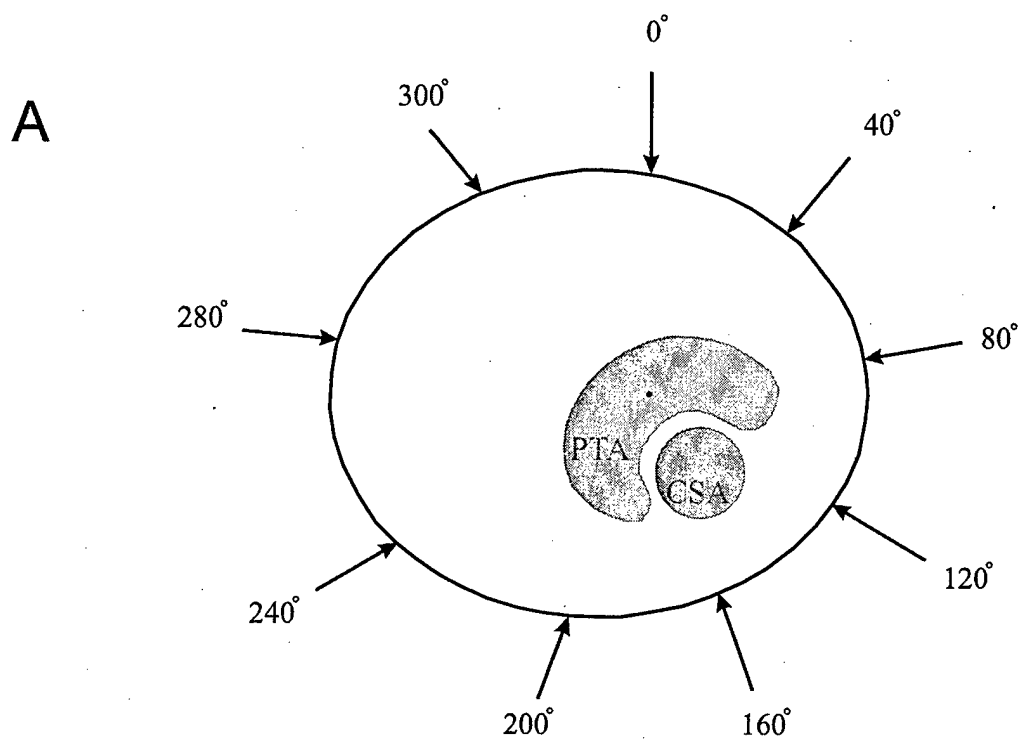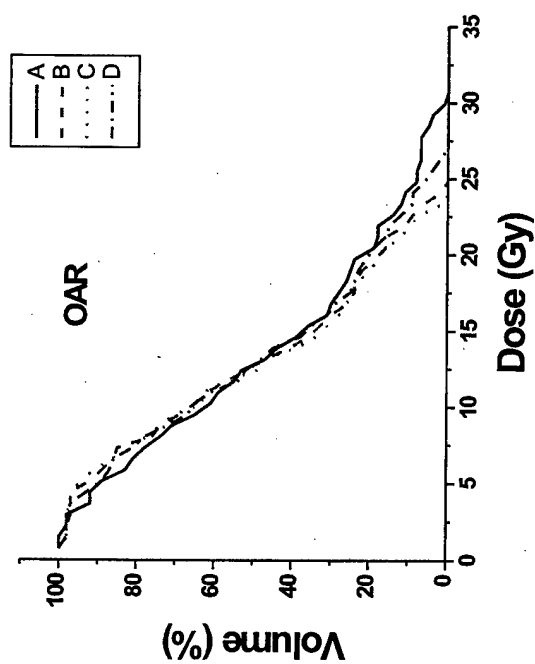
Figure 1

Figure 2

# Target parameter distribution
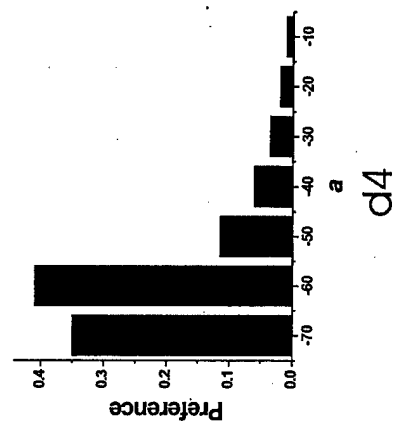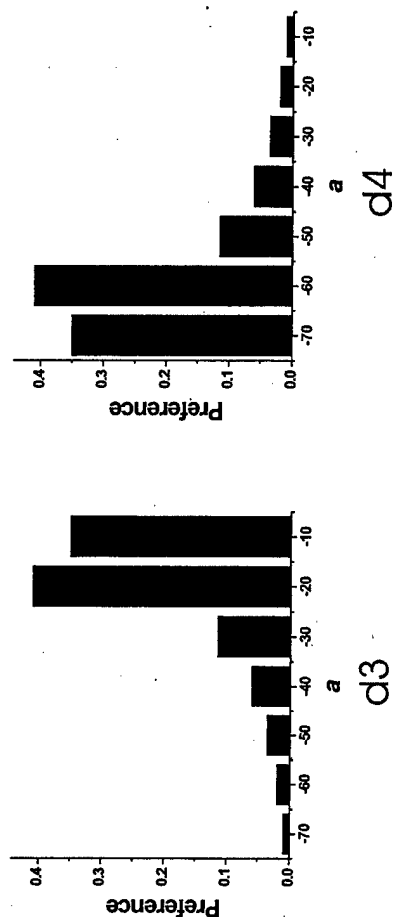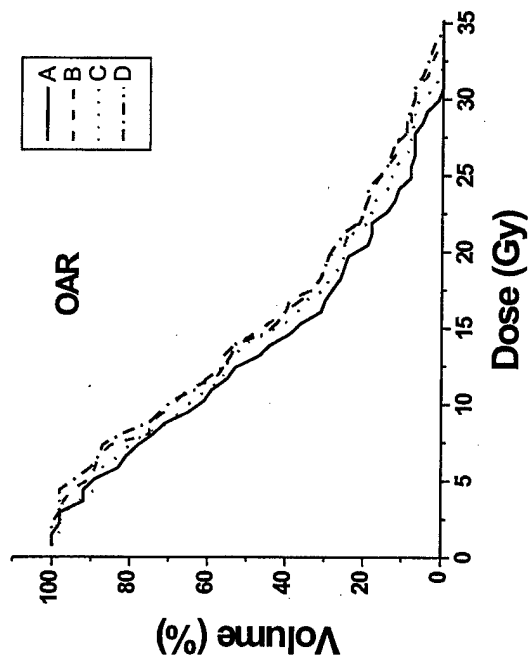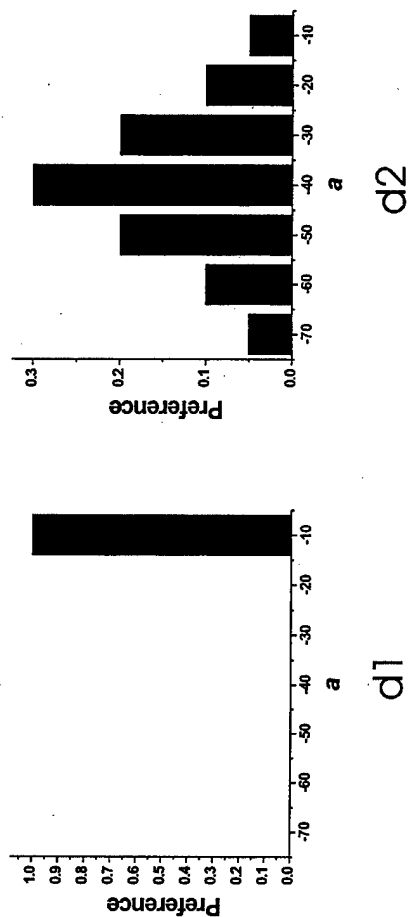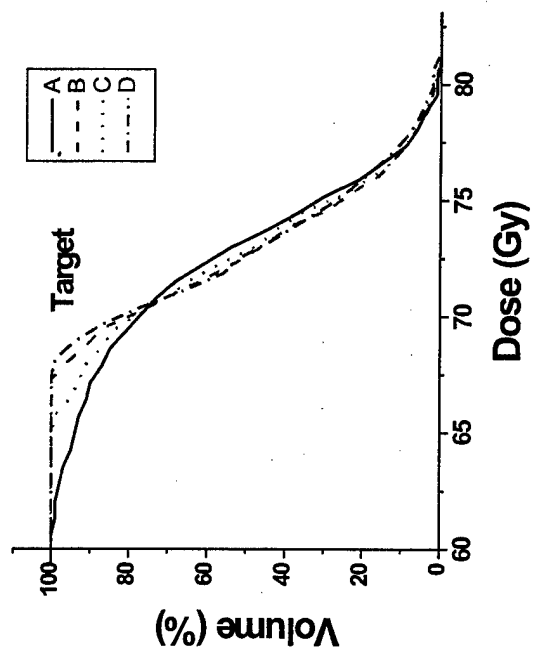


Figure3

A



B
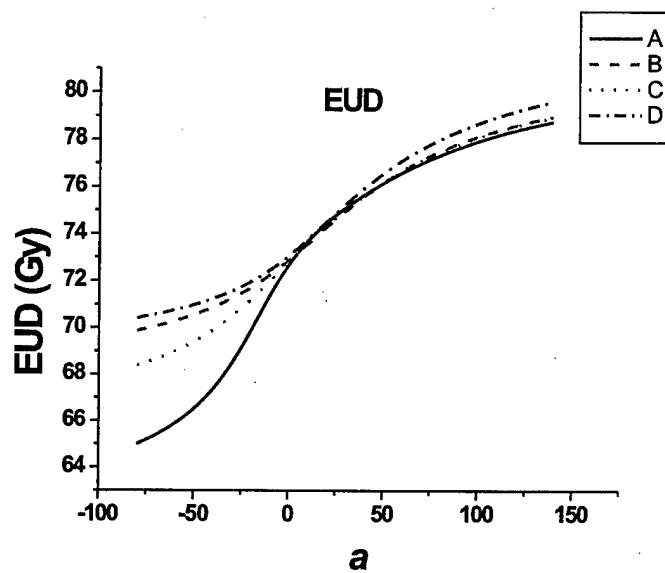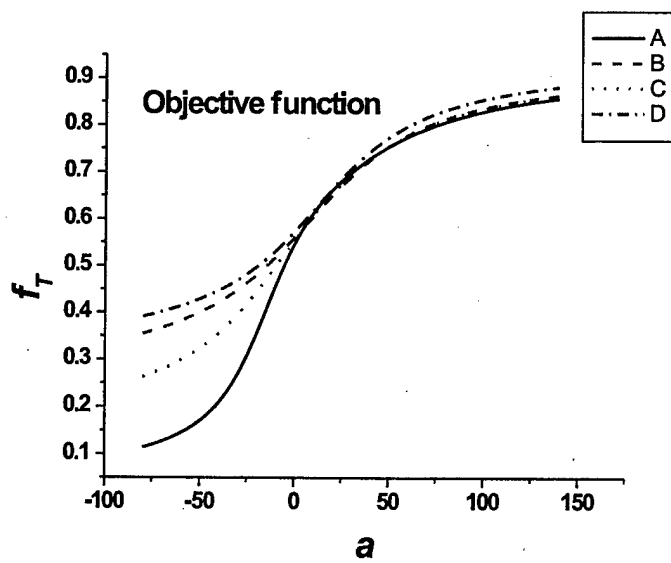


Figure 4
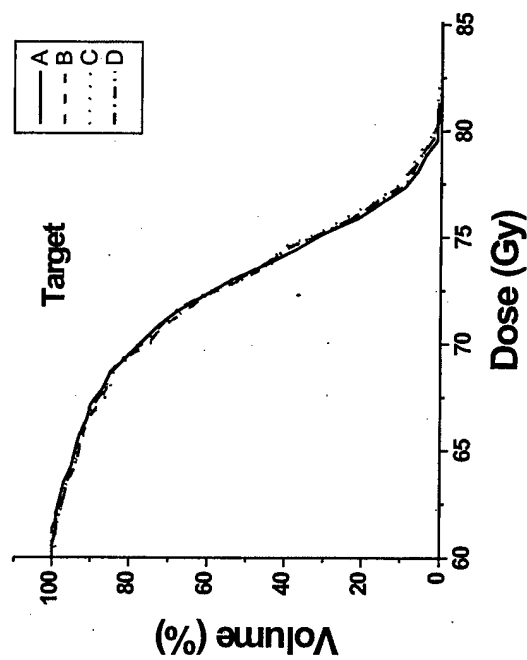
OAR parameter distribution
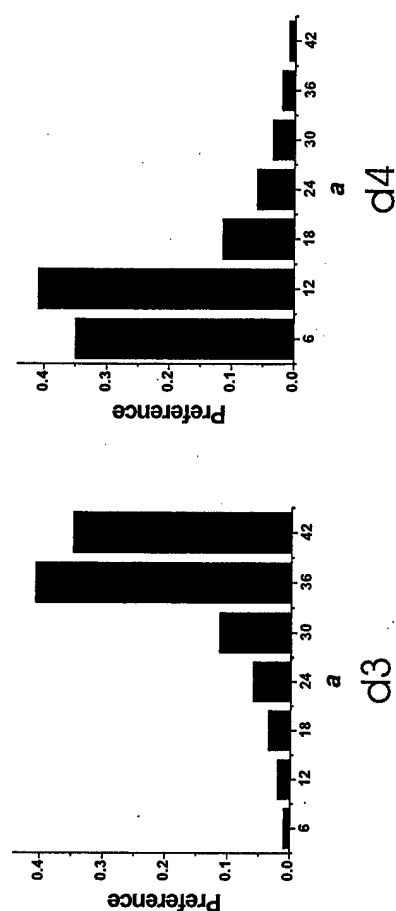
Figure 5

A
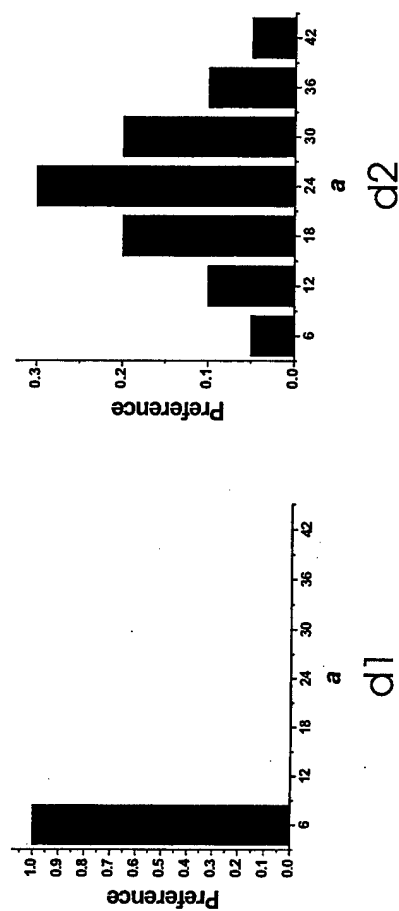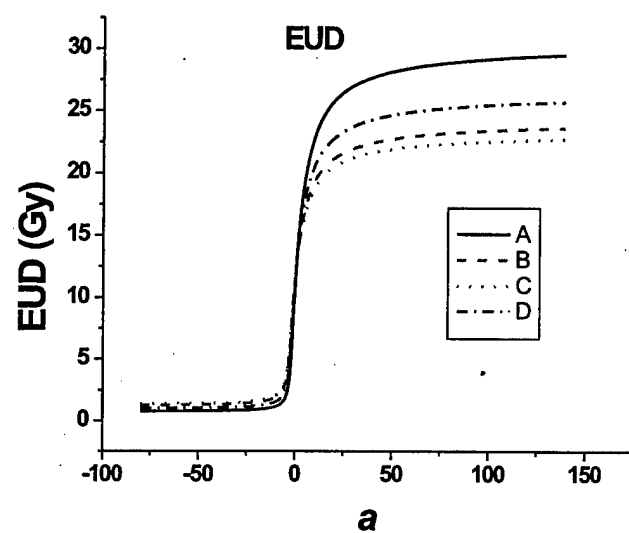


B
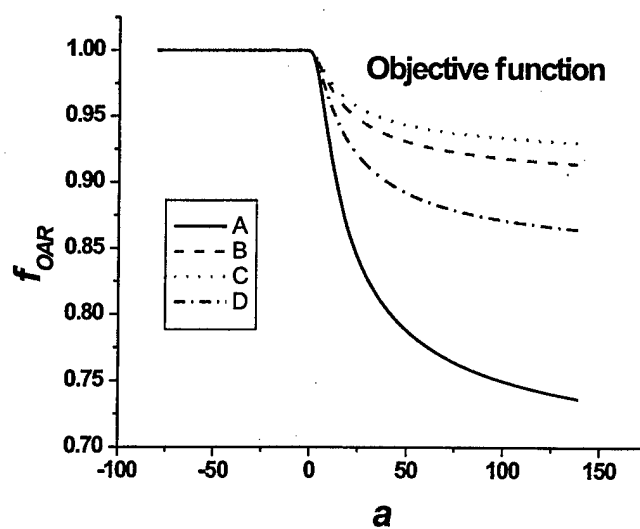
Figure 6

A



B
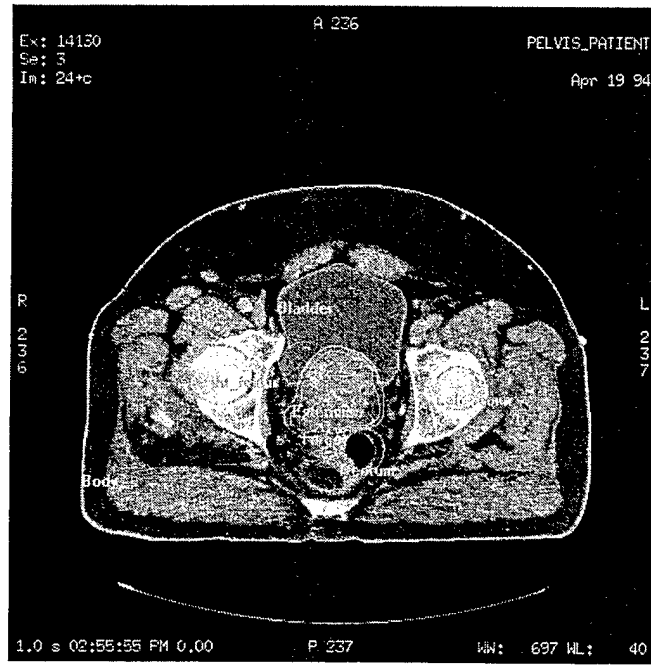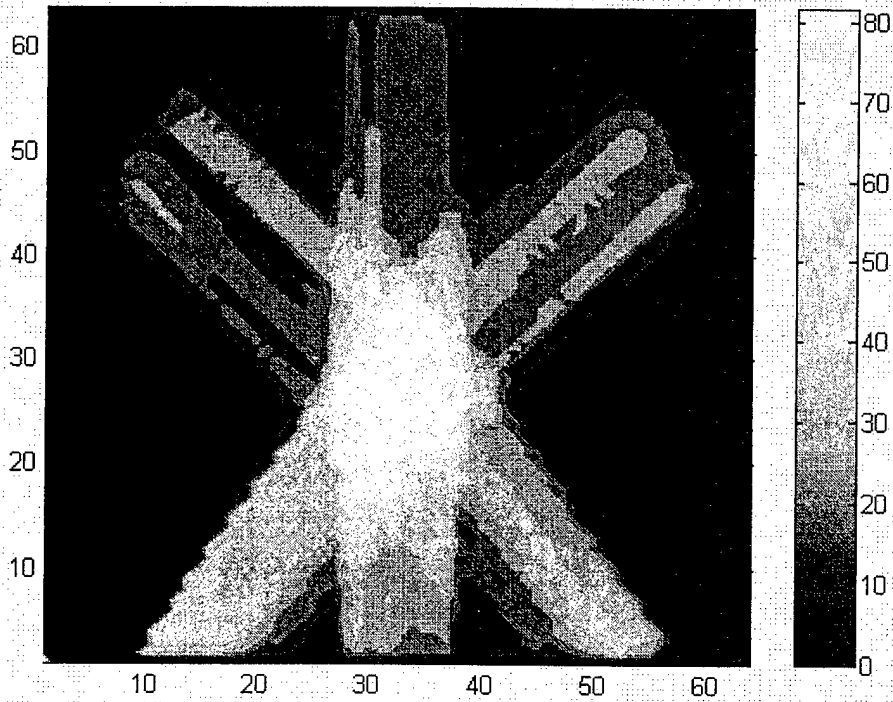


Figure 7
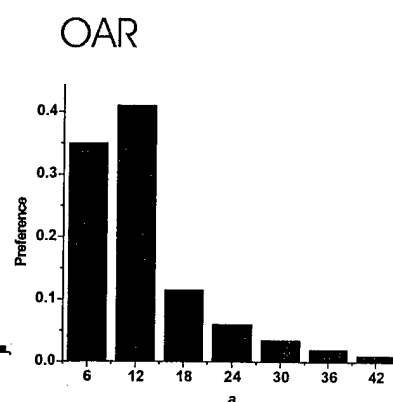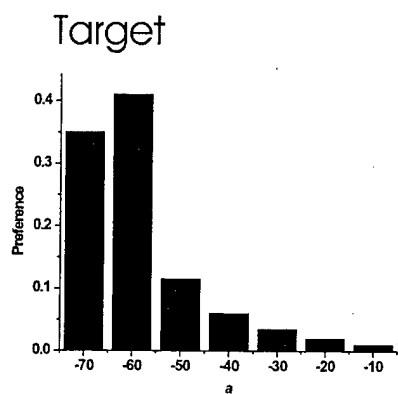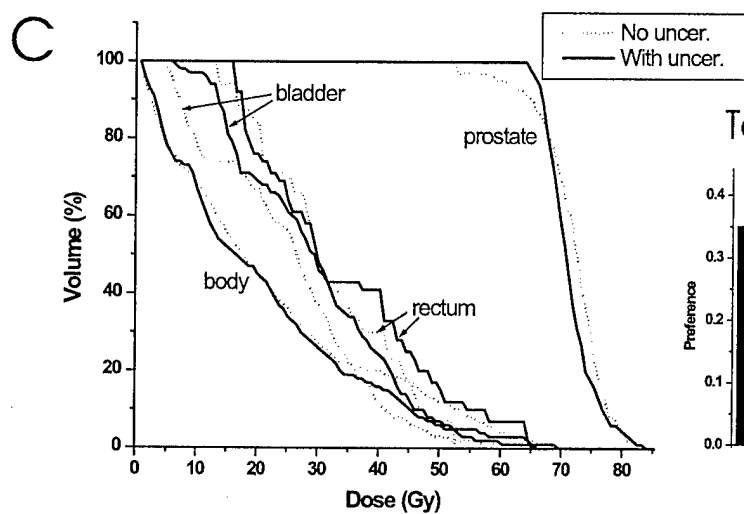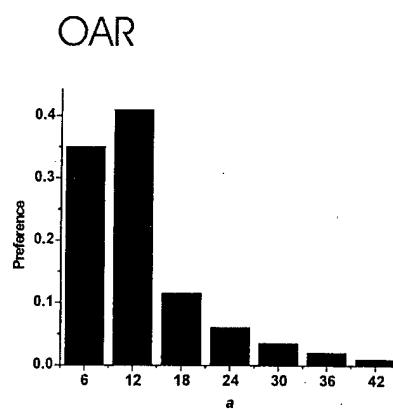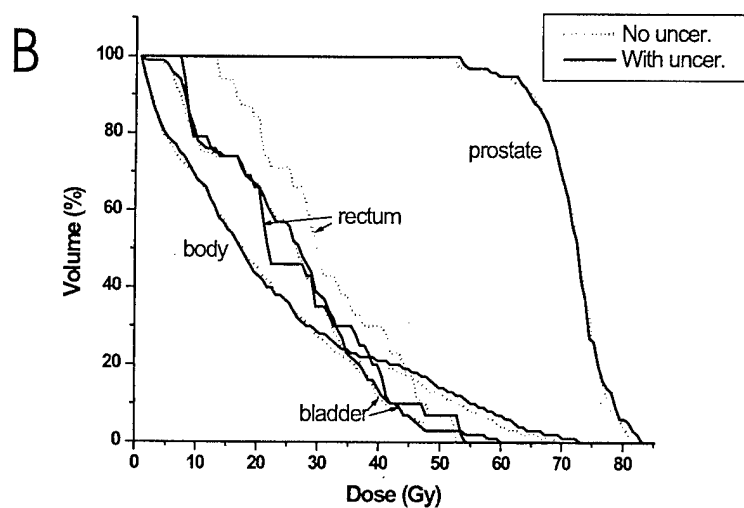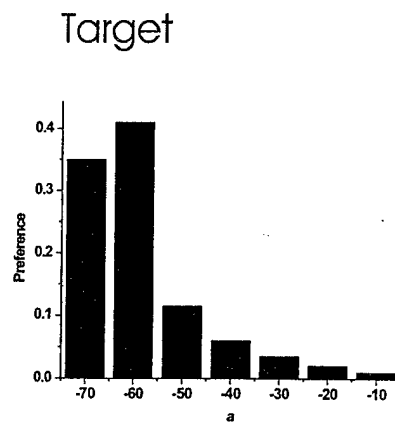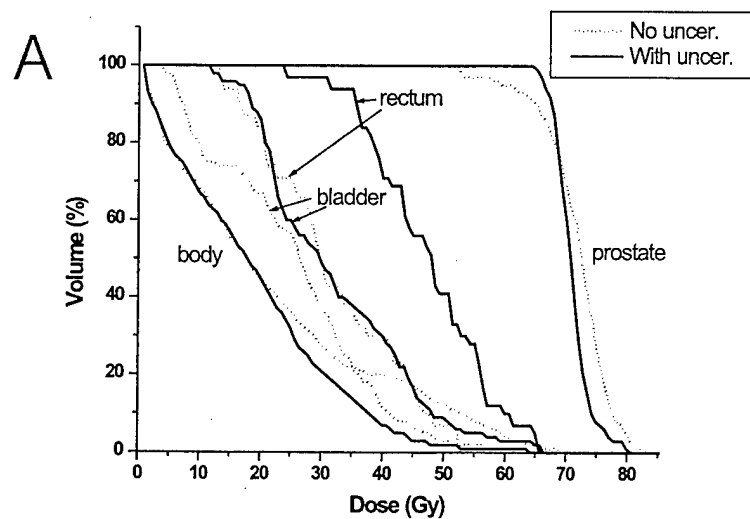
Figure 8
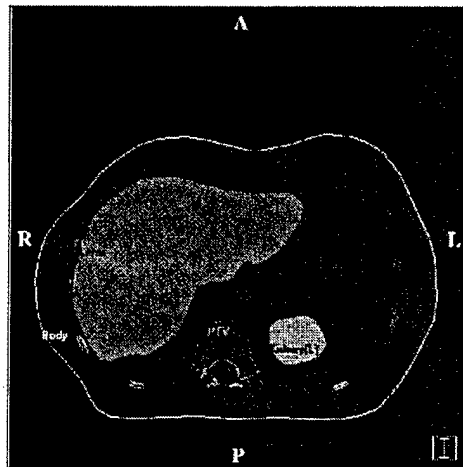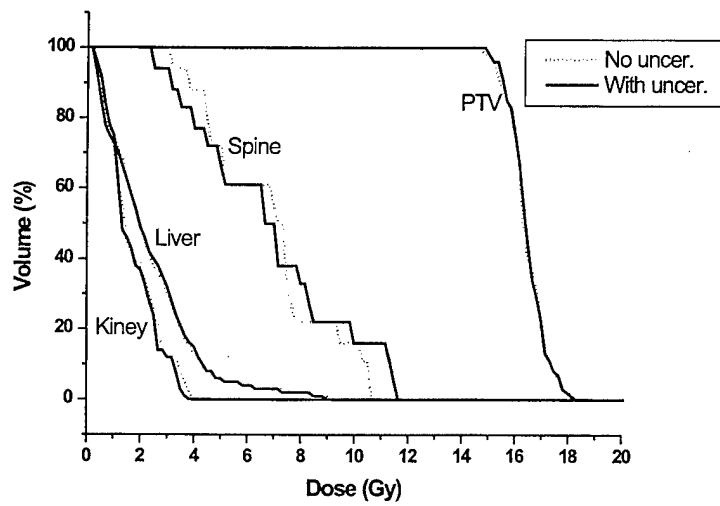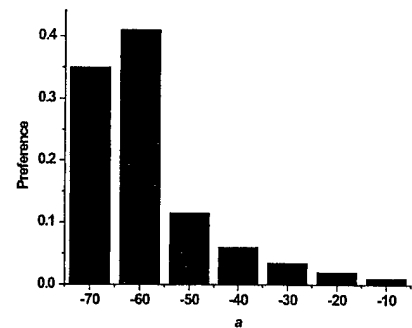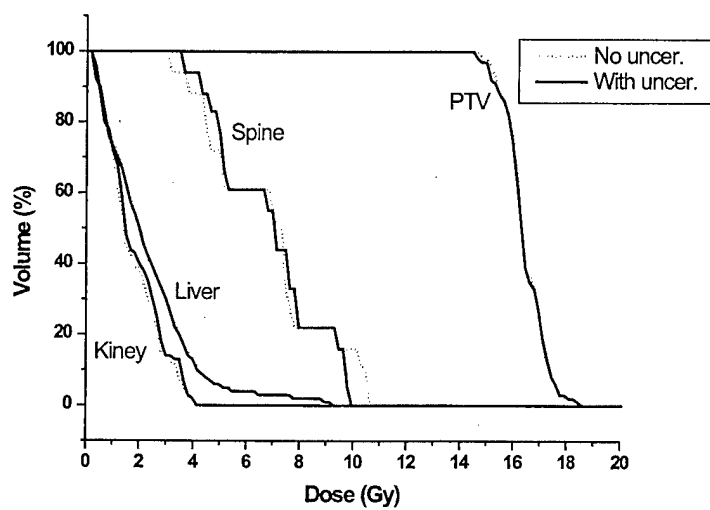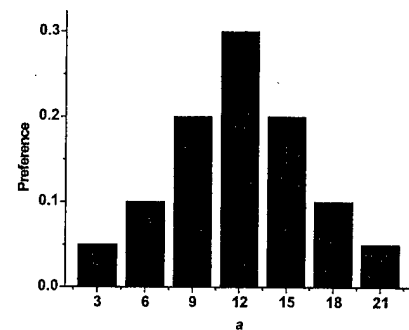
Figure 9

# Biological Model Based IMRT Optimization with Inclusion of Parameter Uncertainty

## Jun Lian[1] and Lei Xing[2]

[1]Department of Radiation Oncology, The University of North Carolina at Chapel Hill, Chapel Hill, NC

[2]Department of Radiation Oncology, Stanford University, Stanford, CA

## Abstract

Radiobiological treatment planning depends not only on the accuracy of the models describing the dose-response relation of different tumors and normal tissues but also on the accuracy of tissue specific radiobiological parameters in these models. Whereas the general formalism remains the same, different sets of model parameters lead to different solutions and thus critically determine the final plan. Here we describe an inverse planning formalism with inclusion of model parameter uncertainties. This is made possible by using a statistical analysis-based frameset developed by our group. In this formalism, the uncertainties of model parameters, such as the parameter $a$ that describes tissue-specific effect in EUD model, are expressed by probability density function and are included in the dose optimization process. We found that the final solution strongly depends on distribution functions of the model parameters. Considering that currently available models for computing biological effects of radiation are simplistic, and the clinical data used to derive the models are sparse and of questionable quality, the proposed technique provides us with an effective tool to minimize the effect caused by the uncertainties in a statistical sense. With the incorporation of the uncertainties, the technique has potential for us to maximally utilize the available radiobiology knowledge for better IMRT treatment.

## Keywords

inverse planning, dose optimization, biological models, IMRT

## Introduction

Most IMRT optimization systems at present use dose and/or dose volume-based objective functions [1, 2], which guide the IMRT planning by imposing a penalty according to the difference between the computed and prescribed doses. A well-known drawback of the dose-based inverse planning is that the nonlinear dose response of tumor or normal structures is not fully considered. A number of mathematical models have been developed over the years to better describe the biological effect of radiation, which include tumor control probability (TCP) [3], normal tissue complication probability (NTCP) [4], equivalent uniform dose (EUD) [5] and the probability of uncomplicated tumor control (P+) [6]. In parallel to these modeling efforts, considerable works have also been done to use these biological models to construct more meaningful objective functions for therapeutic dose optimization [7] .

Generally speaking, radiobiological formalism involves the use of model parameters that are of considerable uncertainty [8]. For instance, the radiosensitivity $\alpha$ of Webb's TCP model varies from 0.157 Gy-1 to 0.090 Gy-1 when model parameters were fit to 103 patients' data [3]. Biological 'margins' have been used to account for the variability in radiation sensitivity. This method assumes the patient to be more sensitive than the mean value for normal tissues and more resistant for the tumor [9]. Kåver et al proposed a stochastic optimization to account for clinical uncertainties, including the varying radiosensitivity [10, 11]. The objective function was constructed based on a linear quadratic Poisson model which approximates the probability of curing the patient or inflicting injury. Two parameters in the model could be calculated if the standard deviation of dose per faction was known. The optimization was thus executed corresponding to different standard deviations.

We have recently presented a general statistical analysis-based inverse planning framework [12, 13] and applied it to investigate the influence of model parameter uncertainties in biologically based dose optimization [14]. The purpose of this paper is to provide a detailed description of the technique and addresses several important issues related to the dose optimization in the presence of model parameter uncertainties. In our approach, the uncertainty of a model parameter is quantified by a probability density function and its influence is then incorporated into inverse planning through the use of a statistical inference theorem [12]. The technique is illustrated by using a hypothetical C-shaped tumor case and a prostate tumor case with an EUD-based model. Considering that currently available models for computing biological effects of radiation are simplistic, and the data they rely on are sparse and of questionable quality, the proposed technique provides us with an effective tool to minimize the effect caused by the uncertainties in a statistical sense. The treatment plans so obtained are generally less sensitive to the inter-patient variation and other types of uncertainties that may otherwise influence the final treatment plan greatly.

## Material and Methods

### Statistical analysis-based inverse planning

The inverse problem as posed for IMRT consists of the determination of the beamlet weight vector *w* when a desired plan is prescribed. In a vectorial form, the dose to the points in the treatment region depend upon the beamlet weights *w* as

$$D_c = d \cdot w, \quad (1)$$

where *d* represents the dose deposition coefficients matrix, expressing the dose deposited to any patient point when irradiated with a unit weight beamlet. The total number of physically realizable dose distributions $D_c$ in IMRT is enormous and increases exponentially with the number of beamlets. Inverse planning is essentially a plan selection process from the vast pool of physically realizable solutions. In a recent paper, Xing *et al* [12] introduced a statistical analysis-based inverse planning technique. In this approach the commonly used objective function is reformulated into a probability density function whose value gives the figure of merit of a dose distribution. A virtue of the approach is that it allows us to obtain solution in the presence of uncertainties of the prescription parameters or other model parameters using a statistical inference technique. Application of the technique to deal with a system with a set of variable dose prescriptions has been described in another work of our group [13]. Here we use the formalism for biological modeling based- inverse planning in the presence of model parameter uncertainties. To be specific, we use an equivalent uniform dose (EUD)-based objective function employed by Wu et al [7] and discuss the consequences of the variation of model parameter *a* and how to incorporate the fluctuations into inverse planning dose optimization to obtain statistically optimal solutions.

### EUD model and EUD-based objective function

The concept of equivalent uniform dose (EUD) for tumor was originally introduced by Niemierko as the biologically equivalent dose that, if given uniformly, would lead to the same cell kill in the tumor volume as the actual nonumiform dose distribution. Recently, Niemierko et al suggested a phenomenological form [5]:

$$EUD = \left( \frac{1}{N} \sum_i D_i^a \right)^{\frac{1}{a}} \quad (2)$$

for both tumor and normal tissues, where $N$ is the number of voxels in the structure, *a* is the tumor or normal tissue-specific parameter that describes the dose-volume effect. EUD described in Eq. (2) is the general mean of the non-uniform dose distribution. According to the mathematic properties of the function [15], for $a = \infty$, the EUD is equal to the maximal dose, and for $a = -\infty$, the EUD is equal to the minimum dose. Tumors generally have large negative values of *a*, whereas serial critical structures (e.g. spinal cord and rectum) have large positive values and parallel critical structures that exhibit a large dose-volume effect (e.g. liver, parotids, and lungs) have small positive values.

The objective function or figure of merit used to measure the goodness of a dose distribution or the corresponding EUD is given by [7]

$$F = \prod_j f_j, \quad (3)$$

where the component subcore $f_j$ may be either

$$f_T = \frac{1}{1 + \left( \dfrac{EUD_0}{EUD} \right)^n} \quad (4)$$

for tumors, or

$$f_{OAR} = \frac{1}{1 + \left( \dfrac{EUD}{EUD_0} \right)^n} \quad (5)$$

for normal tissues and organs at risk (OARs). $EUD_0$ is the desired dose parameter for the target volume and the maximal tolerable uniform dose for normal structures. Parameter $n$ is akin to the structure specific importance factor [16] in the conventional inverse planning formalism that parameterizes our tradeoff strategy of different structure.

### Incorporation of the variation distribution of the model parameter into inverse planning

We assume that $a_k$ in the EUD model varies according to a simple Gaussian distribution

$$P_n(a_k) = P'_{0n} \exp\{-r_n[a_k - a_0]^2\}, \quad (6)$$

where $a_0$ is the mean value, $P'_{0n}$ is a normalization constant and $a_k$ is one of the sampling values of *a*. For a given distribution, the EUD and the corresponding figure of merit of an IMRT plan vary with the sampling of *a*. We thus rewrite Eqs. (4) and (5) as conditional probabilities for a sampled $a_k$:

$$P_T(EUD \mid a_k) = \frac{1}{1 + \left( \dfrac{EUD_0}{EUD} \right)^n}, \quad (7)$$

$$P_{OAR}(EUD \mid a_k) = \frac{1}{1 + \left( \dfrac{EUD}{EUD_0} \right)^n}. \quad (8)$$

The objective function for a structure $m$ in the presence of uncertainty in *a* is expressed as the summation of a series of joint probabilities

$$P_m(EUD) = \sum_k P_m(EUD \mid a_k) \cdot P_m(a_k), \quad (9)$$

and the overall objective function $P$ of the system is a product of $P_m(EUD)$ defined in Eq. (9). That is

$$F = \ln(1/P) = -\ln \prod_m P_m(EUD) = -\sum_m \ln \sum_k P_m(EUD \mid a_k) \cdot P_m(a_k)$$
$$(10)$$

## Results and Discussion

### The C-shaped tumor case

We illustrate the proposed technique by planning a hypothetical IMRT phantom case with a C-shaped target next to a circular critical structure. Nine 6MV equi-spaced beams were used for the treatment (0°, 40°, 80°, 120°, 160°, 200°, 240°, 280°, and 320° – respecting the IEC convention).

The parameter $a$ in EUD model characterizes the dose-volume effect but its value is generally not known accurately even for clinically well studied organs. We first investigated the behavior of the system when the parameter $a$ of the target EUD takes four different distributions, as depicted in the bar charts shown on the right of Fig. 1, while keeping the parameter $a$ of the OAR at a constant $a_0 = 6.0$. In the case shown in Fig. 1A, the parameter $a$ takes only a single value, $a_0 = -10$, which is a simple case studied by Wu et al [7]. The rest of Fig. 1 shows three representative types of distributions of the EUD parameter $a$. For each of these situations we carried out the dose optimization calculation using the method outlined in the last section.

The optimal plans for the four distributions of parameter $a$ differ significantly, as indicated by the target and OAR DVHs shown in Fig. 2. To estimate the degree of sensitivity of the solutions against a variation in $a$, we computed the target EUD and the objective function, $f_T$, as a function of parameter $a$ for the four optimal dose distributions under different types of uncertainty distributions. The results are plotted in the left panel of Fig. 1. For plan A, the EUD changes from 65 to 71 Gy when $a$ is varied from –10 to -70 and to 79 Gy when $a$ is equal to 140. The objective function varies from 0.11 to 0.85 in the range of variation in $a$. For plan D, the EUD is narrowed to a range between 70 Gy and 79 Gy. The EUD variations of plans B and C are similarly reduced. These results suggest that the EUD becomes much less sensitive to the variation in parameter $a$ in the plans obtained with some "built-in" distributions in parameter $a$ (i.e., plans corresponding to Figs. 1B-3D).

The uncertainty of parameter $a$ of the OAR can be similarly included in the dose optimization process when its distribution is known. In the second study, we fixed the target EUD parameter $a = -10$ and allowed the parameter $a$ of the OAR to take four different distributions as plotted in the right of Fig. 3. Once again, we found that the final solution strongly depends on the distributions of the parameter $a$.

In Fig. 4 we plot the target and OAR DVHs for the four possible scenarios shown in Fig. 3. The maximum doses of the OAR of the four plans vary from 24 Gy to 30 Gy. Note that the doses to the OAR in plans B, C and D are less than that of plan A, where the parameter $a$ is restricted to a single value, $a_0 = 6$. This is explainable since the parameters $a$ in plans B, C and D are shifted up to higher values. As $a$ increases, the EUD puts more emphasis on the high dose (recall that EUD becomes the maximum dose when $a = \infty$). As a consequence of the increased "effective" $a$ value in the distributions shown in Figs. 3 B, C and D, the OAR dose is improved in comparison with the plan obtained under the assumption of a fixed $a$ value (Fig. 3A). Interestingly, the target DVHs shows that four distinct plans have very similar target coverage. It is well known that in dose optimization there is generally no net gain: an improvement

in the dose to a structure is often accompanied by a dosimetrically adverse effect(s) at other points in the same or different structures. The result here suggests that, from a clinical point of view, it is possible to have a great gain in one structure with a little sacrifice in another structure. How to find the truly optimal tradeoff represents a practical subject that is worth of studying in the future.

As can be expected from the discussion in previous paragraphs, the solution obtained with $a_0 = 6$ (Fig. 3a) is more sensitive to a variation in parameter $a$. Indeed, as seen from Fig. 3, the EUD for this plan varies from 1 Gy to 30 Gy when $a$ is changed from -80 to 140. On the other hand, the EUD changes for the rest three situations are much less for the same variation in $a$. The upper bound of the EUD is reduced to 26 Gy for plan D, 24 Gy for plan B, and 23 Gy for plan C. The objective functions of four plans show a similar trend.

## Conclusions

We have proposed and implemented a technique for incorporating biological model parameter uncertainties into inverse treatment planning. The formalism is quite general and does not prerequisite the specific form of uncertainty distributions of the involved model parameters. By including model parameter uncertainties, the final solution becomes more robust and the treatment outcome will be less likely influenced by inter-patient variation of biological characteristics. With the increasing interest in radiation therapy community to use biologically based models for treatment planning, this work provides an effective way to better account for the known uncertainties in the model parameters and allows us to maximally utilize the available radiobiology knowledge to facilitate patient care.

## Acknowledgements

## References:

1.      Wu, Q. and R. Mohan, Algorithms and functionality of an intensity modulated radiotherapy optimization system. Med Phys, 2000. 27(4): p. 701-11.

2.      Xing, L., et al., Fast iterative algorithms for three-dimensional inverse treatment planning. Med Phys, 1998. 25(10): p. 1845-9.

3.      Levegrun, S., et al., Fitting tumor control probability models to biopsy outcome after three-dimensional conformal radiation therapy of prostate cancer: pitfalls in deducing radiobiologic parameters for tumors from clinical data. Int J Radiat Oncol Biol Phys, 2001. 51(4): p. 1064-80.

4.      Lyman, J.T., Complication probability as assessed from dose-volume histograms. Radiat Res Suppl, 1985. 8: p. S13-9.

5.      Niemierko, A., Reporting and analyzing dose distributions: a concept of equivalent uniform dose. Med Phys, 1997. 24(1): p. 103-10.

6. De Meerleer, G.O., et al., Radiotherapy of prostate cancer with or without intensity modulated beams: a planning comparison. Int J Radiat Oncol Biol Phys, 2000. **47**(3): p. 639-48.

7. Wu, Q., et al., Optimization of intensity-modulated radiotherapy plans based on the equivalent uniform dose. Int J Radiat Oncol Biol Phys, 2002. **52**(1): p. 224-35.

8. Deasy, J.O., K.S. Chao, and J. Markman, Uncertainties in model-based outcome predictions for treatment planning. Int J Radiat Oncol Biol Phys, 2001. **51**(5): p. 1389-99.

9. Brahme, A., Optimized radiation therapy based on radiobiological objectives. Semin Radiat Oncol, 1999. **9**(1): p. 35-47.

10. Kåver, G., et al., Stochastic optimization of intensity modulated radiotherapy to account for uncertainties in patient sensitivity. Phys Med Biol, 1999. **44**(12): p. 2955-69.

11. Lof, J., B.K. Lind, and A. Brahme, An adaptive control algorithm for optimization of intensity modulated radiotherapy considering uncertainties in beam profiles, patient set-up and internal organ motion. Phys Med Biol, 1998. **43**(6): p. 1605-28.

12. Xing, L., et al., Estimation theory and model parameter selection for therapeutic treatment plan optimization. Med Phys, 1999. **26**(11): p. 2348-58.

13. Lian, J., C. Cotrutz, and L. Xing, Therapeutic treatment plan optimization with probability density-based dose prescription. Med Phys, 2003. **30**(4): p. 655-66.

14. Xing, L., J. Lian, and C. Cotrutz. Inverse treatment planning with inclusion of model parameter uncertainty. in the 44th Annual AAPM Meeting. 2002. Montreal.

15. Abramowitz, M. and I.A. Stegun, Handbook of mathematical functions with formulas, graphs, and mathematical tables. 1984, Wiley-Interscience: New York. p. 1046.

16. Xing, L., et al., Optimization of importance factors in inverse planning. Phys Med Biol, 1999. **44**(10): p. 2525-36.
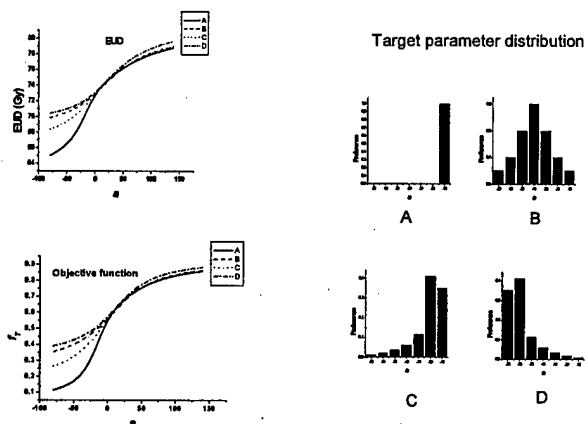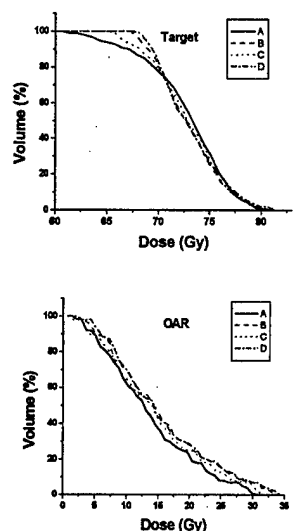
Figure 3:



Figure 4:
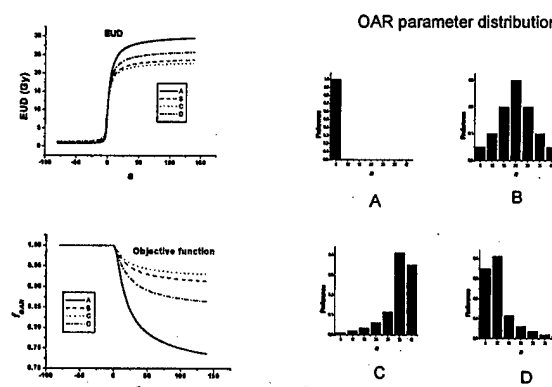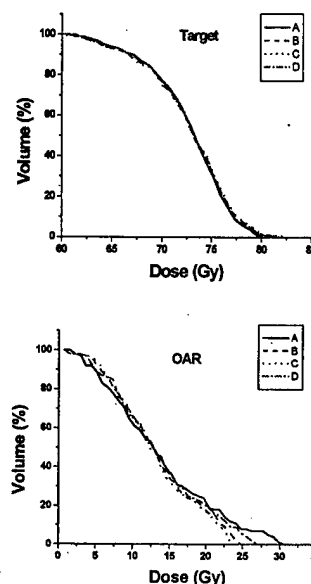
# Figures:

Figure 1:



Figure 2:

# Including Metabolic Uncertainty into Proton MR Spectroscopic Imaging (MRSI)-Guided Inverse Treatment Planning

J. Lian, D. Spielman, C. Cotrutz, S. Hunjan, E. Adalsteinsson, C. King, G. Luxton, A. Boyer, D. Kim, B. Daniel and L. Xing

## Abstract

With the development of functional imaging techniques and intensity modulated radiation therapy (IMRT), there is growing interest in image-guided IMRT to produce customized 3D dose distributions in accordance with the patient specific biological requirements. MRSI is one of the most promising functional imaging modalities and has been applied to brain, breast, and prostate cancer imaging. In practice, however, the MRSI data do not always accurately reflect the actual metabolic level over the entire imaging volume due to our limited ability to shim near air-filled cavities and/or the strong dependence of the surface coil SNR on the spatial position. In this work, we provide an algorithm to numerically incorporate the spectral uncertainties into MRSI-guided IMRT treatment planning. Assuming that the fluctuation of the spectral activity or the prescribed dose $EUD_0(n)$ at voxel $n$ is specified by a probability distribution $P_n(EUD_0)$, we treat $P_n(EUD_0)$ as *a priori* variable distribution and construct an objective function based on the statistical inference technique. The algorithm is used to plan a phantom case with hypothetical functional distributions and a brain tumor treatment with incorporation of MRSI and the corresponding confidence map. The results indicated that the proposed technique is capable of producing deliberately non-uniform dose distributions consistent with the MRSI and its spatial uncertainty distribution. Considering that currently available functional image data are not completely reliable and that missing spectral data may occur frequently, the proposed technique provides us with an effective tool to minimize the effect and generate statistically optimal treatment plans.

# Including Metabolic Uncertainty into Proton MR Spectroscopic Imaging (MRSI)-Guided Inverse Treatment Planning

## Introduction

MRSI is one of the most important functional imaging modalities and has been applied to brain, breast, and prostate cancer imaging. The modality can not only be used to more accurately delineate the tumor target but also reveals tumor biology distribution that allows us to identify high/low tumor burden regions. The imaging data are thus potentially useful to guide radiation therapy treatment planning to produce deliberately non-uniform dose distribution that selectively boosts the high tumor burden regions. In practice, however, the MRSI data do not always accurately reflect the actual metabolic level over the entire imaging volume due to our limited ability to shim near air-filled cavities and/or the strong dependence of the surface coil SNR on the spatial position. In this work, we provide an algorithm to numerically incorporate the spectral uncertainties (confidence map) into MRSI-guided IMRT treatment planning. The new formalism is based on the Bayesian statistical inference theorem. For illustration purpose, a EUD model is used as the plan ranking function. The method is applied to study a phantom case with a few hypothetical functional distributions and a brain tumor case with inhomogeneous tissue abnormal levels indicated by a ratio of Choline and NAA from MRSI.

## Methods

The equivalent uniform dose (EUD) is the biologically equivalent dose that, if given uniformly, would lead to the same cell kill in the structure as the actual non-uniform dose distribution. It is defined as:

$$EUD = \left( \frac{1}{N} \sum_i D_i^a \right)^{\frac{1}{a}}$$

for both tumor and normal tissues, where $N$ is the number of voxels in a structure, $a$ is the tissue-specific parameter that describes the dose-volume effect. Assuming $EUD_0(n)$ is the voxel desired dose parameter and it is linearly related to tissue metabolic level $M(n)$ (Cho/NAA in brain tumor). We postulate

$$EUD_0(n) = EUD_0^c(n) + kM(n)$$

for a tumor, where $EUD_0(n)$ is the desired dose at voxel $n$, $EUD_0^c(n)$ is the conventional prescription dose and $k$ is an empirical coefficient. Similarly $EUD_0(n)$ for a critical structure is defined linearly proportional to a functional importance factor. In this way, the uncertainty of measured biological data can be projected into a $EUD_0$ distribution function. Given a value of $EUD_0$, our preference over the occurrence of the EUD can be expressed as a conditional probability,

$$P_T(EUD \mid EUD_{0k}) = \frac{1}{1 + \left( \dfrac{EUD_{0k}}{EUD} \right)^n},$$

$$P_{OAR}(EUD \mid EUD_{0k}) = \frac{1}{1 + \left( \dfrac{EUD}{EUD_{0k}} \right)^n},$$

for target and organ at risk, respectively. The uncertainty in $EUD_0/M(n)$ can be cast into the objective function or the preference function of the system based on Bayesian theorem. The preference can be modeled as the summation of a series of joint probabilities:

$$P_n(EUD) = \sum_k P_n(EUD \mid EUD_{0k}) \cdot P_n(EUD_{0k})$$

The overall preference function $P$ of $N$ voxel system is a product of $P_n(EUD)$.

## Results

The method was applied to an IMRT treatment of malignant glioma. The target metabolic map was discretized into three levels (Fig. A) based on the values of choline/NAA ratio. In a conventional plan, the inner region with highest abnormality (target 1) was prescribed 64 Gy, the middle region (target 2) 54Gy and the external region (target 3) 44 Gy. Because the measurement of choline/NAA has great uncertainty, we replaced the fixed

value desired dose ($EUD_0$) with a probability density based dose prescription. For instance, the target 1 was prescribed 58,60,62,64,66,68,and 70Gy with probabilities 12%, 13%,16%,18%, 16%, 13% and 12% respectively. A dose distribution is shown in Fig. B when three targets are all prescribed with a Gaussian type distribution. The objective functions are lower than those of the conventional plan (Fig. C). The corresponding DVH shows this type of distribution could result in slight under dose (Fig. D), suggesting a higher dose prescription may be needed when measurement uncertainty is of a Gaussian form. Target DVHs highly depend on the distribution of the abnormity levels. Assuming target 3 needs to be prescribed with higher probabilities for doses less than 44 Gy, and target 1 needs to be prescribed with higher probabilities for doses over 64 Gy, we found the resultant DVHs were significantly different than those of a conventional plan (Fig. E).

## Conclusions

We have used functional MRSI metabolic data to guide the design of IMRT treatment plan. The uncertainty represented in functional imaging has been integrated into the dose optimization. Using this algorithm, the effects of the MRSI spectral uncertainty can be minimized in a statistical sense and functional data can be used more efficiently and accurately.

## Figures

A)

B)

C)



D)

E)



A) Three targets (1, 2 and 3) with different abnormality indicted by MRSI. B) Dose distribution with inclusion of Gaussian type uncertainty. Target 1, 58 to 70Gy, target 2, 48 to 60Gy and target 3, 38 to 50Gy, all with 2 Gy intervals. The probability distributions are 12%, 13%, 16%, 18%, 16%, 13% and 12% for seven discretized dose levels. C) Target objective functions for dose prescription stated in B. D) Target DVHs corresponding to dose prescription stated in B. E) Target DVHs corresponding to probability distributions: target 1,1%, 2%, 3%, 39%, 21%, 18%, and 16%; target 2, 12%, 13%, 16%, 18%, 16%, 13% and 12%; target 3, 16%, 18%, 21%, 39%, 3%, 2%, and 1%. Discretized dose levels are the same as in B.